

**Application of Raman spectroscopy for study of
nitrogen containing compounds for astrobiological
purposes**

**Aplikace Ramanovy spektrometrie pro studium látek
obsahujících dusík pro účely astrobiologie**

Ph.D. thesis



Adam Culka

Prague 2011

Charles University in Prague, Faculty of Science

Thesis supervisor

Jan Jehlička

ACKNOWLEDGEMENTS

Main financial support for this study was provided by the grant no. 133107 '*Testování astrobiologických geoindikátorů života pomocí Ramanovy mikrospektroskopie*' (principal investigator M.Sc. Kateřina Osterrothová) from the Grant Agency of Charles University in Prague, additional funding was provided by the grant no. 210/10/467 (principal investigator Prof. Jan Jehlička) from the Czech Science Foundation.

My personal thanks go primarily to my supervisor Jan Jehlička for his expert guidance and patience throughout the whole of my PhD study. I would like to express my gratitude to Ivan Němec from the Department of Inorganic Chemistry for many expert counsels, especially in the field of infrared spectroscopy. Furthermore, I wish to thank Howell G. M. Edwards from the University of Bradford, UK, for his scientific and linguistic help provided for my publications.

Last but not least, I want to thank my family for their irreplaceable support throughout my university studies.

STATEMENT OF ORIGINALITY

I herewith affirm that this PhD thesis represents original results of my own research and that all the resources used in the thesis are properly cited.

I confirm that none of this research work or any of its significant portions was used to acquire any academic degree elsewhere.

In Prague, April 2011

M.Sc. Adam Culka

Institute of Geochemistry, Mineralogy and Mineral Resources

Faculty of Science, Charles University in Prague, Czech Republic

ABSTRACT

This PhD thesis was focused on the evaluation of the application of Raman spectroscopy as an analytical method used specifically for research on selected nitrogen containing compounds in experiments, that are important in the astrobiological context. The results of experiments provided insight into the advantages as well as the limitations of the method in several applications that are expected to be encountered in the future planetary exploration missions with astrobiological context use, and where the Raman spectroscopy is proposed as an advantageous method.

The Raman spectroscopy was tested in various experimental tasks. Several nitrogen containing minerals were analysed, where the features such as the indestructive analysis, small laser spot size, and selection of the excitation source enabled to acquire spectra of minerals even with miniature sample sizes, also the band assignment was published for the first time for some of the studied minerals. Artificially prepared samples of biomarkers mixed in mineral matrices were analysed to test the ability of the method to analyse complex mixtures: three biomarkers and two evaporitic minerals were analysed with a portable instrument, and all compounds were unambiguously detected. When the samples contained more of the similar compounds with many closely occurring bands, such as amino acids, the portable instrument was able to detect and unambiguously distinguish up to five compounds. The measurements with the aim to determine the lowest possible concentration level of selected biomarkers dispersed in the evaporitic mineral matrices were performed both by micro Raman and portable instrumentation. The concentrations of the nitrogen containing compounds that Raman spectroscopy was able to detect in the mineral matrices were generally quite high, in the contrast to, for example, the carotenoid pigments. The lowest concentration detected was for the aromatic heterocyclic nucleobases in the gypsum matrix: 0.1 wt%. This type of experiments also confirmed that the laser spot size had the significant effect on the resulting data. Additionally, the ability of Raman spectroscopy to acquire spectra of satisfactory quality, when analysing samples through the transparent crystals of several evaporitic minerals, was found to be of great importance. Besides the outdoor testing of different types of portable spectrometers, the performance these instruments demonstrated in the difficult Alpine winter conditions was found to be convincing. Good quality spectra in agreement with the references were obtained for samples including pure solid compounds, ices of nitrogen containing compounds, minerals and biomarker-mineral mixtures. Results of several distinct experiments carried out in this work proved that Raman spectroscopy, in properly selected instrumentation, should be able to perform the scientific tasks related to the planned missions with astrobiological and geochemical focus and provide unique and high valued information about the measured samples.

ABSTRAKT

Předkládaná disertační práce se zaměřuje na vyhodnocení využití Ramanovy spektrometrie jako analytické metody pro výzkum vybraných dusík obsahujících látek v experimentech, které jsou důležité z hlediska astrobiologie. Výsledky experimentů poskytují cenné informace o výhodách a omezeních metody při řešení úkolů a problémů, které jsou očekávány v průběhu plánovaných výzkumných misí se zaměřením na astrobiologii, kde je Ramanova spektrometrie považována za jednu z velmi platných výzkumných metod.

Ramanova spektrometrie byla testována v různých experimentálních úkolech: Při analýzách dusík obsahujících minerálů, díky svým vlastnostem, jako nedestruktivní analýza, malá velikost stopy laseru a možnost výběru zdroje excitačního záření, metoda umožnila získat kvalitní data; spektra některých zkoumaných minerálů byla interpretována a publikována vůbec poprvé. Analýzami uměle připravených vzorků směsí biomarkerů a minerálů byla zkoumána použitelnost metody pro analýzu složitějších směsí: ve směsi třech biomarkerů a dvou minerálů byly všechny složky jednoznačně detekovány. V případě detekce biomarkerů, například aminokyselin, ve směsi podobných sloučenin, s množstvím pásů, přenosný spektrometr byl schopen rozlišit až pět podobných sloučenin. Dále byly prováděny analýzy za účelem zjištění, jaké nejnižší koncentrace biomarkerů rozptýlených v minerálních vzorcích jsou schopné detekovat laboratorní mikrospektrometr a přenosný spektrometr. Zjištěné koncentrace pro většinu testovaných dusík obsahujících sloučenin byly obecně relativně vysoké, v porovnání například s pigmenty typu beta-karoten. Nejnižší dosažená koncentrace jedna desetina hmotnostního procenta byla zjištěna v případě detekce sloučenin nukleových bází rozptýlených v minerálu sádrovci. Tento typ experimentů také prokázal významný vliv velikosti stopy laseru na výsledná data. Dále byla zkoumána schopnost Ramanovy spektrometrie při měření prováděné skrz průhledné krystaly minerálů jako sádrovec a kalcit a byly zjištěny dobré výsledky. Kromě testování různých typů přenosných přístrojů v terénu byly prováděny měření v nepříznivých vysokohorských zimních podmínkách s výbornými výsledky. Kvalitní spektra byla získána při analýzách čistých látek, ledů dusík obsahujících sloučenin, minerálů a připravených směsí biomarkerů a minerálů. Výsledky experimentů získané při zpracování této práce dokládají, že Ramanova spektrometrie, při použití vhodné instrumentace, by měla být schopná provádět a řešit vědecké úlohy a problémy, které nepochybně vyvstanou při plánovaných průzkumných misích se zaměřením na astrobiologii a geochemii, a přinášet unikátní a vysoce důležité informace o studovaných vzorcích.

TABLE OF CONTENTS

| | |
|--|-----|
| ACKNOWLEDGEMENTS..... | II |
| STATEMENT OF ORIGINALITY..... | III |
| ABSTRACT | IV |
| ABSTRAKT | V |
| TABLE OF CONTENTS | VI |
| 1. INTRODUCTION..... | 7 |
| 2. NITROGEN CONTAINING COMPOUNDS | 8 |
| 3. APPLICATION OF VIBRATIONAL SPECTROSCOPY WITH FOCUS ON THE ASTROBIOLOGICAL AND GEOLOGICAL TASKS | 18 |
| 4. INSTRUMENTAL AND EXPERIMENTAL..... | 26 |
| 5. RESULTS | 29 |
| 6. DISCUSSION | 46 |
| 7. GENERAL CONCLUSIONS | 55 |
| 8. REFERENCES..... | 56 |

APPENDICES

A Culka A., Jehlička J. and Němec I., Raman and Infrared Spectroscopic Study of Boussingaultite and Nickelboussingaultite, *Spectrochimica Acta Part A: Molecular and Biomolecular Spectroscopy*, 73 (2009) 420-423. (Elsevier)

B Culka A. and Jehlička J., Raman microspectrometric investigation of urea in calcite and gypsum powder matrices, *Journal of Raman Spectroscopy*, 41 (2010) 1743-1747. (Wiley)

C Culka A., Jehlička J., Edwards H. G. M., Acquisition of Raman spectra of amino acids using portable instruments: Outdoor measurements and comparison, *Spectrochimica Acta Part A: Molecular and Biomolecular Spectroscopy* 77 (2010) 978-983. (Elsevier)

D Culka A., Jehlička J., Vandenabeele P. and Edwards H. G. M., The detection of biomarkers in evaporite matrices using a portable Raman instrument under Alpine conditions, *Spectrochimica Acta Part A: Molecular and Biomolecular Spectroscopy*, doi:10.1016/j.saa.2010.12.020 (Elsevier)

1. INTRODUCTION

1.1 Astrobiology

Astrobiology (also known as exobiology) is a relatively new science field. Like many other newly established science fields astrobiology developed from a neglected science to a fully acknowledged field of research. The growing significance of astrobiology was in direct connection with the significant progress in the space exploration missions that started in the 1960' and it brought many questions that needed to be answered. As an interdisciplinary science astrobiology combines the knowledge from many established science disciplines such as: chemistry, astronomy, physics, biology, planetary science, geology, molecular biology, ecology, engineering. Its field of interest is so wide that it encompasses very different tasks: e.g. the Search for Extra-Terrestrial Intelligence program and the studies of microorganisms living in the hydrothermal vent environment at ocean floor. Astrobiology mainly focuses on problems involving origin of life, searching for traces of life at extraterrestrial places, looking for habitable environments.

1.2 Aims and implications of this work

This work focuses on the application of vibrational spectroscopy with the emphasis on Raman spectroscopy for the detection and analysis of nitrogen compounds in various astrobiology related settings. These compounds are very important since organic molecules containing nitrogen are the very basic building blocks needed for a life (as we know it) to exist. Raman spectroscopy as a main research method was chosen because it has a great potential for ongoing as well as future astrobiological research. Providing indestructive detection and analysis, it is designed to be one of the scientific instruments for the planned planetary exploration missions with focus on astrobiology.

The major goals of this research work were:

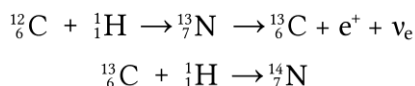
1. To acquire and interpret Raman spectra of selected nitrogen containing minerals that can be formed in the geological settings especially those of them that are formed in the presence of the decomposing organic matter

2. To assess the potential of Raman spectroscopy for the detection of selected nitrogen containing biomarkers on qualitative and if possible quantitative basis. In the scope of this work the experimentally prepared mixtures of biomarkers in the mineral matrix will approximately represent natural samples, to see to which extent is Raman spectroscopy able to collect valuable data. The tasks will be selected to cover both detection limits of biomarkers and distinguishing between biomarkers in more complex mixture of similar compounds

3. To evaluate commercially available portable Raman instruments in the outdoor measurements experiments starting at relatively easy conditions at measurement sites to experimentally difficult high altitude winter measurements which serve better as an approximation for the Raman instrument on a rover for the planned planetary exploration missions

2. NITROGEN CONTAINING COMPOUNDS

Nitrogen is the seventh most abundant chemical element in our Galaxy with fraction of 960 parts per million in the hydrogen and helium dominated universe according to Croswell (1996) and fifth according to Lewis (2004). Vast majority of nitrogen was (and is being) created in the second generation or younger stars through the mechanism called CNO cycle. In this process protons are burnt in series of nuclear reactions to produce helium and energy. The reactions involving the production of nitrogen isotopes are:



Equation 1

This process also occurs in our Sun, but due to its relatively small mass the energy production of the Sun is dominated by other reaction called proton-proton chain reaction process. Nitrogen has two stable isotopes ^{14}N (99.636% of all nitrogen) and ^{15}N and several unstable isotopes usually with very short half-lives with the exception of ^{13}N that has half-life of about 10 minutes.

Nitrogen (and therefore nitrogen containing compounds) is relatively rare on Earth when the whole planetary mass is considered. This is probably due to the fact that light, volatile molecules (H_2 , He, NH_3 , CH_4) were accumulated more in the outer solar system. The largest reservoirs (by mass) of nitrogen are nitrogen in rocks: $1.9 \cdot 10^{23}$ g, Earth's atmosphere $3.9 \cdot 10^{21}$ g, in sediments $4 \cdot 10^{20}$ g, N_2 dissolved in ocean $2.2 \cdot 10^{19}$ and about 10^{18} g of nitrogen in organic matter and living biomass both oceanic and terrestrial (Söderlund and Svensson, 1976). Total mass of Earth is approximately $6 \cdot 10^{27}$ g.

Aside from the most common and the most chemically stable nitrogen compound in the atmosphere and hydrosphere, the molecular N_2 , other simple molecules are present in reservoirs: N_2O , NO_3^- , NH_4^+ , NO_x , originating either from natural processes such as lightning or from the biological activity (including significant anthropogenic contribution). The majority of these nitrogen compounds are involved in the biogeochemical nitrogen cycle that consists of fundamental processes, such as nitrogen fixation, nitrification and denitrification. Nitrogen global cycle is no less important than the carbon cycle for the existence of life on Earth.

2.1. Naturally occurring organic nitrogen containing compounds

As one of the biogenic elements, nitrogen is an essential element for the life as we know it. In the process of nitrogen fixation the N_2 is transformed into its reduced form NH_3 (or NH_4^+) that can be directly utilised by the autotrophic organisms for further biosynthesis of nitrogen containing organic compounds that make up a significant part of total organic biomass. In the following paragraphs, the most important groups of nitrogen containing organic compounds will be reviewed with the focus on the naturally occurring compounds since the utilisation of nitrogen containing compounds utilised in the modern organic chemistry and industry is immense.

Amines

The most important and the most widely occurring nitrogen-containing organic compounds in biological organisms are amines. Amines are basically organic derivatives of ammonia (NH_3). Chemically can be amines classified based on the number of organic substituents replacing the hydrogen atoms attached to central nitrogen atom. Primary amines have one organic group attached to the nitrogen, secondary amines two, and tertiary amines the maximum of three (Figure 1). The lone pair of electrons on the nitrogen atom results in the basicity of amino group.

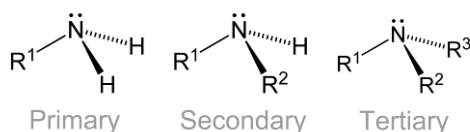


Figure 1 Amines classification

The organic substituents R_1 - R_3 can be either alkyl or aromatic aryl groups. The majority of naturally occurring amines have complex molecules, but some simple aliphatic amines or polyamines are known, such as putrescine and cadaverine, products of amino acids breakdown, and spermidine important in cellular metabolism (Lawrence, 2004). An example of a simple cyclic naturally occurring amine is piperidine which is also a heterocyclic compound from alkaloid group. Other biologically substantial amines, such as amino acids and nucleobases will be discussed below.

Amides

Amides are derivatives of carboxylic acids where the $-OH$ group is replaced by the $-NH_2$ group or other amine. Amides are the most stable derivatives of carboxylic acids in the conditions occurring in the living organisms (McMurry, 2008). The simplest amide is formamide (methanamide) it is also one of the two simplest molecules containing all essential biogenic elements C, H, N and O, a fact that is important for prebiotic

astrobiological studies. Barks et al. (2010) were able to produce purine nucleobases adenine, guanine and hypoxanthine by UV irradiation of formamide solutions. Urea (carbonyl diamide) is an important waste product of amino acids metabolism.

Nitriles

Nitriles are nitrogen-containing compounds containing $\text{—C}\equiv\text{N}$ functional group. They are frequently prepared and used in the organic chemistry but examples of natural occurring compounds are also known. Cyanogenic glycosides are used by some plants for storage of the poisonous cyanide group (that can be released using enzymes) as a natural defense mechanism against animal pests and herbivores (Gleadow et al., 1998). Cyanocycline A, an antibiotic isolated from bacteria (Hayashi et al., 1982) contains a nitrile group in addition to the nitrogen heteroatoms in its structure.

Heterocyclic compounds containing nitrogen

Other very important organic compounds are heterocyclic compounds that contain one or more heteroatoms (atoms other than carbon and most commonly nitrogen, oxygen or sulphur) in their carbon ring structure. They can be distinguished by the number of atoms in the ring (usually 3 - 7), number of heteroatoms, whether they are saturated or unsaturated (aromatic), whether the lone electron pair is part of the aromatic system or not, and by number of rings. The five to six member ring or fused ring heterocyclic compounds are common structural units in the biological compounds, good example is the complex group of alkaloids (good examples are coniine, nicotine, caffeine). The fact, that alkaloids can be used as drugs, led to the synthesis of a great number of similar compounds for pharmaceutical use (some antibiotics, pyrazine, piperazine). The simplest nitrogen containing aromatic heterocyclic molecule is pyrrole. Four pyrrole molecules are the backbone for macrocyclic pigment molecules both in animal cells (porphyrin, heme) or plants or bacteria (chlorophylls, bacteriochlorines). Lone electron pairs of the heterocyclic nitrogen atoms are used for bonding of a central ion (Fe^{2+} in case of heme, Mg^{2+} in case of chlorophylls). Bilirubin, a heme metabolite, is an example of tetrapyrrole that is not macrocyclic. Phthalocyanines, artificially prepared widely utilised pigments, are structurally somewhat similar but feature isoindole instead of pyrrole subunits.

Nucleobases

Pyrimidine (=1,3-Diazine) is an aromatic heterocyclic six-membered ring that has three very important derivatives: cytosine, thymine and uracil. Purine is somewhat more complex heterocyclic aromatic molecule consisting of two fused six and five membered rings each containing two nitrogen atoms. Its most important derivatives are adenine and guanine but other purine-like compounds have important biological use (uric acid).

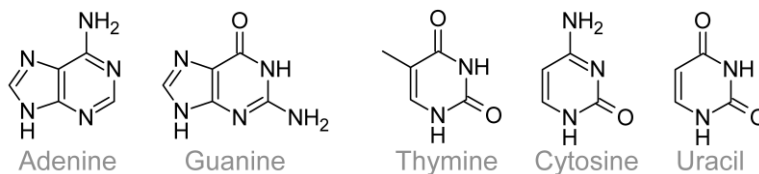


Figure 2 Purine and pyrimidine derived nucleobases

These compounds (Figure 2) are essential for life to exist, because they are a basic building blocks of nucleic acids DNA and RNA giant macromolecules that carry the genetic code in each living organism on Earth. Each nucleobase is connected through a glycosidic bond to a five carbon monosaccharide ribose or deoxyribose in the cyclic form to form a *nucleoside* and via an ester bond to one to three phosphate groups to form a *nucleotide* that polymerise to form one strand of nucleic acid. The nucleobase sides of the two strands of DNA (or RNA) are bonded through hydrogen bonds to form complementary base pairs (adenine always bonds to thymine or uracil, and guanine always bonds to cytosine). The succession of these pairs in the strand is where the genetic information is stored. The sequence of three nucleobases is called codon and usually codes a unique amino acid.

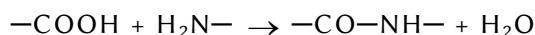
Adenosine triphosphate is another example of essential biomolecule serving as a basic unit of energy that is used in the cellular metabolism that has a purine backbone. Of these nucleobases, adenine, 6-aminopurine, is the heterocyclic molecule that is structural fundament for the great number of naturally occurring biomolecules (molecules that have very different function for example uric acid and caffeine) and that could be directly formed in the prebiotic conditions by '*condensation of five HCN molecules without any further external instructions*' (Rosemeyer, 2004).

Amino acids

The genetic information encoded by the use of nucleobases needs to be transformed into basic building blocks for other more complex molecules that the living organisms are very much made of, or need them to metabolise or propagate themselves. These building blocks are amino acids, relatively small and simple molecules consisting of H, C, N, O occasionally other elements, such as sulphur, are also essential (methionine, cysteine). Their unique property is that all amino acids contain in their molecules at least one amino group —NH_2 which is slightly basic and at least one —COOH group which is slightly acidic. In many amino acids the distribution of electrons may result in the appearance of a formal electric charges on a different atom groups (usually on NH_3^+ and COO^-) and although the molecule is electrically neutral as a whole, it behaves as an 'inner ion', *zwitterion*. This form has an impact on the characteristics of a molecule and notable differences in the vibrational spectra can be observed when amino acid is in this form. All α -amino acids (that have carboxylic and amino group attached to the same carbon) except glycine have asymmetric (chiral) carbon atom with four different substituents and are

optically active (can rotate a plane of polarisation of passing light). The most interesting fact is that all living organisms utilise only the so called L form of amino acids in the contrast with the racemic (mixtures of half L and half R) amino acids are found for example in the extraterrestrial samples such as meteorites. This ultimate choice of the organic life to use exclusively L forms of amino acids along with the sole utilisation only of R saccharides is not yet understood and may be traced to the very beginning of life.

Through condensation reaction and a water molecule elimination a covalent chemical bond is formed between the acid and basic groups:



Equation 2

These peptide bonds allow the low amino acid polymers *peptides* to be made. Polymerisation of peptides results into *polypeptides* and ultimately to the huge molecules called *proteins* consisting of tens to thousands of amino acids with median length of 361 amino acids for eukaryotes (Brocchieri and Karlin, 2005). Such big molecules usually fold into globular three dimensional objects or form filaments whose primary (amino acid sequence) to quaternary (way how proteins form structural aggregates) structures determine the function of the protein. Proteins have various crucial functions in the organism: building and structural, enzymatic, transmitter and others.

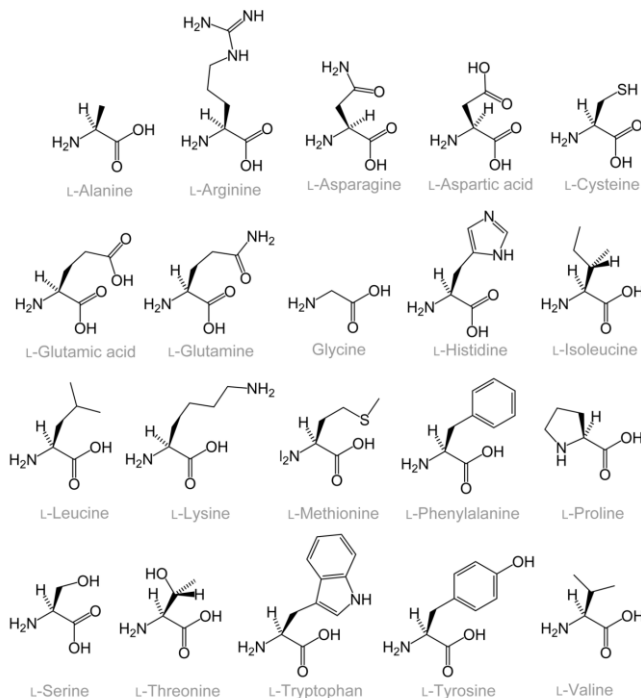


Figure 3 Proteinogenic amino acids

Amino acids can be categorised for example by the overall acidic or basic behaviour, whether they are linear or branched, hydrophilic or hydrophobic. These different chemical characteristics ensure the wide use of amino acids in the organism. Of all α -amino acids, 20 amino acids (Figure 3) are proteinogenic (they are used by the genetic code and are building blocks for all proteins). These are glycine, alanine, glutamic acid, glutamine, arginine, aspartic acid, asparagine, serine, histidine, proline, tyrosine, cysteine, valine, leucine, isoleucine, phenylalanine, threonine, lysine, methionine and tryptophan. Eight of these are considered essential for humans, that means human cells cannot synthesise them and they have to be acquired in the nourishment: valine, leucine, isoleucine, phenylalanine, threonine, lysine, methionine and tryptophan. Organisms can use various compounds to synthesise amino acids, rats were shown to utilise even diammonium citrate and urea as a source of nitrogen (Rose et al., 1949).

In addition to the 20 proteinogenic amino acids more than 700 non-proteinogenic amino acids (McMurry, 2008) are found in nature where they perform important tasks. All higher animals need to dispose of excessive nitrogen that is a waste product of the amino acids metabolism. Usually animals living in water environments excrete ammonia due to the great solubility in water and lesser energy costs. Birds and reptiles use uric acid as an end product of metabolism (evolutionary developed strategy to save more water during the excretion). In human urine the most common nitrogen containing compound is urea with much less concentrations of uric acid and creatinine (end product of muscle metabolism). All these compounds were detected by laser Raman spectroscopy in human urine (Premasiri et al., 2001).

There is also a growing group of natural compounds, usually secondary metabolites called mixed metabolites that contain fragments of structurally different molecules that contain nitrogen. For example terpenoid hydrocarbons contain commonly only C, H, O atoms but for example agelasine, a sponge metabolite, consist of labdane fragment connected to a heterocyclic ring structure (Kharitonov et al., 2006). Or simply, functional groups such as $-\text{CN}$ or $-\text{NHCHO}$ are contained in those natural molecules (Alvi et al., 1991). These compounds are also very important because of their antimicrobial properties or other pharmaceutical usage.

2.2 Nitrogen containing minerals

This section will review the most important occurrences of minerals containing either NH or NH_4 group, in the geological environment. The source of nitrogen in these minerals can be either of biological origin (e.g. decomposition of organic matter) or the geological origin (e.g. ammonia rich fluids in active volcanic areas). New mineral phases or minerals are found also at the anthropogenic locations such as burning coal heaps, waste dumps and similar localities. A new phase of $(\text{K}, \text{NH}_4)\text{MgCl}_3 \cdot 6\text{H}_2\text{O}$ was identified in a repository for low level radioactive waste in a former salt mine (Herbert et al., 1995) that is different from ammonium bearing carnallite at the same locality (Siemann, 1994). Aromatic organic mineral kladnoite $\text{C}_6\text{H}_4(\text{CO})_2\text{NH}$, a naturally occurring phthalimide that crystallises

on coal waste heaps was discovered near Kladno, Czech republic (Rost, 1937). Raman spectra of kladnoite were acquired and interpreted by Jehlička et al. (2007).

Nitrogen containing organic minerals

Organic minerals oxalates, salts of oxalic acid, can be found in the geological environment and can act as biomarkers. They are formed in the biological processes (e. g. in lichens) and for example whewellite, Ca-oxalate can be found in the sedimentary and coal series as a product of decomposition of organic matter (Leavens, 1968). Frost et al. (2003) used FTIR and Raman spectroscopy and Raman spectroscopy at 77 K (Frost and Weier, 2003) for detection of natural oxalates, implying that oxalates might be suitable biomarkers of primitive life forms (lichens and fungi). Oxammite, ammonium bearing oxalate was found by Winchell and Benoit (1951) in bat guano deposits. Detailed thermogravimetry and Raman spectroscopic study was published by Frost and Weier (2004).

Abelsonite (Figure 4), a purple coloured crystalline nickel porphyrin mineral with a probable composition $C_{31}H_{32}N_4Ni$ was found in the Green River Oil shale formation, Utah, USA (Milton et al., 1978). It belongs to the group of petroporphyrins, highly interesting group of mineral biomarkers occurring in the oil bearing rocks derived from the chlorophyll pigments of the buried organic matter. Its structure was discussed by Storm et al. (1984), but the exact type of chlorophyll that is a precursor to abelsonite was not established unambiguously.

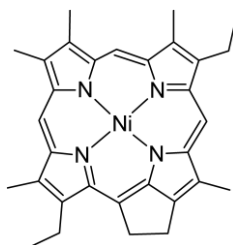


Figure 4 Structure of porphyrin abelsonite

Nitrogen containing phosphate minerals

Another distinct group of minerals that contain NH_4 group are phosphate minerals, specifically those of this group named 'cave' minerals. Many minerals of this group have been found in the complex paragenesis as a result of processes ongoing in the decomposition of bat guano deposits. Struvite, newberyite and hannayite were studied by Raman spectroscopy by Frost et al. (2005). Secondary sulphate minerals were also reported to originate in the process of bat guano breakdown: taylorite, mascagnite, aphthitalite, lecontite, and oxammite (Winchell and Benoit, 1951). A Raman spectroscopic characterisation of lecontite, $(NH_4)Na(SO_4) \cdot 2H_2O$ was conducted by Kloprogge et al. (2006).

Nitrogen containing borate minerals

Ammonia containing borate minerals were found in the boric acid-rich fumarols and lagoons in Larderello, Tuscany, Italy. Both ammonioborite $(\text{NH}_4)_2[\text{B}_5\text{O}_6(\text{OH})_4]_2 \cdot \text{H}_2\text{O}$ (Schaller, 1933) and its dimorph larderellite $(\text{NH}_4)\text{B}_5\text{O}_6(\text{OH})_4$ (Clark and Christ, 1959) belong to the group of hydrated pentaborates. Barberiite NH_4BF_4 , ammonium tetrafluoroborate is formed in a highly acidic environment and it is stable only under the temperatures of its creation, such as hundreds of degrees Celsius at Fossa crater on Vulcano, Italy (Garavelli and Vurro, 1994).

Ammonia containing minerals also occur in the alunite-jarosite series represented by the formula $\text{AR}_3(\text{SO}_4)_2(\text{OH})_6$ where A refers to cations such as K^+ , Na^+ , and NH_4^+ and R refers to trivalent Fe^{3+} (jarosites) and Al^{3+} (alunites) cations. NH_4 rich alunites are formed on Earth in for example in volcanically active environments at temperatures $< 100^\circ\text{C}$ and $\text{pH} < 2$ (Altaner et al., 1988) or during the oxidation of the sulfide minerals (Dill, 2001). The renewed interest in the jarosite minerals has been caused by the discovery of jarosites on planet Mars by the Mars exploration rover Opportunity (Madden et al., 2004). This discovery implies that liquid water was present in the past on surface of Mars. Alunites were analysed by Raman spectroscopy by Frost et al. (2006a).

Ammonia containing silicate minerals

Ammonia is known to substitute (due to its suitable ionic radius: 1.43 angstrom and its unit charge) other monovalent cations such as Na^+ and K^+ in minerals in igneous rocks such as alkali feldspars (Barker, 1964). The distinction between a new mineral or merely an enriched existing mineral is the question of definition. Just a few minerals of this group are known: Buddingtonite, ammonium feldspar was thought to result from the alteration of plagioclase with ammonium rich hot spring water (Erd et al., 1964). Buddingtonite $\text{NH}_4\text{AlSi}_3\text{O}_8$ of similar composition was found in completely different geological settings in the early Tertiary Condor Oil shale deposit in Queensland, Australia (Loughnan et al., 1983). Ammonioleucite $(\text{NH}_4)\text{AlSi}_2\text{O}_6$ has been found to replace analcime in green dolomitised crystalline schist of the Sanbagawa metamorphic belt, Japan (Hori et al., 1986) and characterised by the IR spectroscopy (Andrut et al., 2004). Other example might be tobelite, ammonium dioctahedral mica found in the kaolinite deposit Tobe, Japan (Higashi, 1982).

2.3 Occurrence of nitrogen containing organic compounds in astrobiological context

Ammonia NH_3 is the simplest common molecule containing reduced nitrogen. It belongs, together with methane CH_4 , water H_2O , nitrogen N_2 , carbon oxides CO and CO_2 , hydrogen H_2 and helium He to the group of primary constituents of all planetary or lunar atmospheres in the solar system. The oxygen rich Earth's atmosphere is an exception due to the constant replenishing of reactive oxygen by photosynthetic organisms. Ammonia NH_3 is the fourth most abundant molecule in the atmosphere of

Jupiter and during the photochemical reactions, mainly hydrazine N_2H_4 is created as well as other products (NH_4CN , NH_4SH) (Lewis, 2004).

Titan

Ammonia is believed to be main constituent of the Saturn's subnebula from which Saturn's satellite Titan accreted. NH_3 thus served as a source for Titan's present nitrogen-dominated atmosphere. The temperature is crucial factor in the stability of a volatile molecule like ammonia. For example comparable sized moons of Jupiter, Ganymede and Callisto were too close to the Sun and not enough ammonia rich ices were available to form their atmospheres (Owen et al., 2006). Evidence was presented for condensed NH_3 as a frost or possibly a fog on or near the surface associated with current geologic activity. This suggests that Titan's nitrogen production processes continue today (Nelson et al., 2009). Actual models presume that Titan's crust is composed of water ice or methane clathrates. The haze condensate is probably hydrocarbon-based, comprising mainly methylacetylene (C_3H_4), and diacetylene (C_4H_2) with other unsaturated hydrocarbons and nitriles such as C_2H_2 , C_2H_4 , HCN , CH_3CN , HC_3N , C_4N_2 and cyanogen (C_2N_2). There is a high probability that meteorites impacting the icy surface enabled complex materials interactions with carbonaceous matter; possibly carboxylic and amino acids formed through meteorite interaction with liquid water and liquid NH_3 (Artemieva and Lunine, 2003, 2005). The biggest reservoir of ammonia on Titan is believed to be the probable 'ocean' under the ice layer. Tobie et al. (2005) based the Titan internal structure model on the coupled thermal and orbital information with the following internal structure: The silicate core with radius of 1900 km is surrounded by high pressure mainly water ices, above that is the ocean layer tens of kilometres thick that is covered by the low density water ice I_h up to the surface. Main sources of heat required to allow the liquid ocean are proposed: radiogenic decay in the core and tidal heating (Grasset et al., 2000). The chemical composition of the ocean in conjunction with temperature conditions was modelled by Lunine and Stevenson (1987) that suggested that $\text{NH}_3 - \text{H}_2\text{O}$ eutectic liquid is possible and attainable at the temperatures as high as 240 K. This is quite high a temperature compared to the 94 K surface temperature. The heat sources needed to warm the ocean to such a temperature are yet to be confirmed, but the already known data suggest, that the ocean can be the best place to look for the possible life. In his paper Fortes (2000) reviews the characteristics of such an ocean from the astrobiological point of view and concludes that conditions such as composition, temperature, pressure, pH and nutrient availability are compatible with microbial life and gives examples of terrestrial microorganisms living under similar conditions. For the existence of interesting molecular chemistry of the Titan surface material from the astrobiological perspective (will be discussed below) is however required a more reactive element such as carbon. Main carbon reservoir on Titan is in the form of methane. Concentration of methane in Titan's atmosphere is (1.6%) (Niemann et al., 2005) which is enough material for the complex chemistry together with the absence of oxygen. Methane, a volatile gas, tends to accumulate in the outer solar system either in the planetary atmospheres or is condensed in the surface ices. Although the occurrence of

detectable amounts of methane on the terrestrial planets is rare, it can be important from the astrobiological point of view. The simultaneous presence of oxygen and methane is a strong indicator of biological activity (Turnbull et al., 2006). Trace amounts of methane were detected in the Martian atmosphere in 2003 that could be of a biological origin (Mumma et al., 2009). While methane is present in the atmospheres of all gas giants in the Solar system, the most interesting methane bearing body is undoubtedly Titan, Saturn's largest moon. The complex methane cycle seems to be well-developed on the present Titan resembling the hydrological cycle on Earth (Atreya et al., 2006). Data from Huygens probe show canal like structures and high surface relative methane humidity, Mitri et al. (2007) calculated that surface hydrocarbon lakes covering just 0.002 to 0.02 of the whole surface would explain the observed values. The methane loss from its atmosphere, due to photochemistry and condensation on the surface, is constantly replenished from the interior (one of possible proposed methane sources is the serpentinisation geological process). McKay and Smith (2005) have proposed a microbial production source of Titan's methane, which is isotopically heavy, however the isotopic values of $^{12}\text{C}/^{13}\text{C}$ are somewhat ambiguous, according to Niemann et al., 2005.

The more complex nitrogen containing organics, most importantly amino acids, are of relevance in astrobiology. Exogenous amino acids (glycine, beta-alanine, alanine) were found in carbonaceous chondritic meteorites of the CM group (Botta et al., 2002; Glavin et al., 2006). Since the classical (Miller, 1953) experiment in the synthesis of amino acids and related compounds under the simulated conditions of primitive Earth, many diverse experiments have yielded amino acids under a variety of conditions. Protein and non-protein amino acids were synthesised under the simulated conditions of interstellar matter (McPherson et al., 1987; Briggs et al., 1992) or in the acid treated tholins (Khare et al., 1984, 1986). Glycine, alanine and urea were detected even in experimentally prepared hydrogen cyanide polymers that are proposed to be a component of the dark matter especially on cometary bodies (Matthews et al., 2006). The interstellar ice grains settings were simulated by Bernstein et al. (1995, 2002) and they found that under those conditions from the simple ices of H_2O , CO , CH_4 , NH_3 , CH_3OH etc. At low temperature of 10 K, organic, yellow coloured substance is produced by UV. This material contains moderately complex organic molecules such as ethanol, formamide, acetamide, hexamethylene-tetramine and after acidic hydrolysis this substance yields common amino acids. To simulate conditions of icy material in the Solar system, Hudson et al. (2008) used ion irradiation on H_2O and CH_3CN ices and found amino acids with estimated yield of 0.1% in the reaction products after hydrolysis. Based on the Urey-Miller experiment Sagan and Khare (1979) conducted first experiments in simulated Titan's and Triton's atmospheres and were able to reproduce the conditions needed for tholin synthesis in laboratory. The reddish-brown product of plasma discharges (tholin) in gas mixtures simulating Titan's atmosphere, have been considered a good analogue to Titan's tholin. This tholin was characterised by PY-GC-MS analysis and alkanes, alkenes, nitriles, aromatic hydrocarbons and nitrogen heterocyclic molecules were found. Urea and up to 16 amino acids were also isolated from acid-treated Titan tholin (Khare et al., 1984, 1986). Tholins are heterogeneous

mixtures of chemical compounds with a complex polymer-like inner structure; they are formed by solar ultraviolet and solar wind irradiation of simple organic molecules such as methane and ethane in the oxygen-free atmosphere. Nutrient potential of tholins was tested by Stoker et al. (1990) and they found that a wide variety of common soil bacteria is able to metabolise synthetically prepared tholins as a carbon source. The two main sources of tholins in our solar system are the largest moons of two gas giants, Saturn's Titan and Neptune's Triton. Titan's atmosphere consists almost entirely of N_2 (98.4%) and CH_4 (1.6%) (Niemann et al., 2005) with trace amounts of other gases, the atmospheric pressure is 1.5 bar and the with CH_4 mole fraction (mixing ratio) gradually increasing to reach the maximum at the surface: 0.49 (Niemann et al., 2005; Thompson et al., 1992) and an average surface temperature of 94K. Triton possesses a much less dense nitrogen atmosphere (around 16 μ bar) with a CH_4 mole fraction only about 10^{-5} at the surface (Broadfoot et al., 1989) and average surface temperature of 38K. Simple organic molecules are generated by photolysis of methane and consequent radical reactions in the stratosphere. Newly created radicals react with atmospheric molecules, including nitrogen and hydrogen and the formation of larger molecules through a series of photolysis and subsequent reactions including polycyclic aromatic hydrocarbons and nitrile (C–N–H) species (Atreya et al., 2006). These hydrocarbons condense and form hazes in the atmosphere.

3. APPLICATION OF VIBRATIONAL SPECTROSCOPY WITH FOCUS ON THE ASTROBIOLOGICAL AND GEOLOGICAL TASKS

Since the discovery of the Raman scattering in the early 20th century, the new type of radiation was discovered independently by Raman and Krishnan (1928) in the liquids and by Landsberg and Mandelstam (1928) in the crystalline matter, the Raman spectroscopy was recognised by a wide scientific community and the application of the effect spread to many areas in science, technology and industry. The biggest stimulation for the development of Raman spectroscopy was the discovery of the source of coherent monochromatic light (lasers). First laser was constructed by Maiman (1960). This allowed a fundamental improvement both in the quality and the quantity of the data that could be acquired from Raman spectra. Raman spectroscopy is a unique analytical method. It allows a fast and unambiguous identification of a sample (when appropriate reference Raman data is available). The analysis can be completely non-destructive, which is important for analyses of samples of biological origin susceptible for example to thermal degradation. The method is capable of identification both of organic and inorganic compounds in the same sample (a desirable feature in astrobiology), when the appropriate excitation source is used. It provides information both about the chemical composition and a structure of studied compound. The latest trends in Raman spectroscopic instrumentation are specialisation (many subtypes of Raman spectroscopy taking advantage of new physical and chemical phenomena are developed: Surface Enhanced Raman Spectroscopy, Resonance Raman spectroscopy, Hyper Raman and many other to further extend the area

of application) and miniaturisation. The last criterion is quite important since it allows the construction of portable or handheld instruments that have virtually limitless potential of application and, thank to the low weight, also allows a feasible utilisation of Raman spectroscopy as an analytical method for the planetary exploration missions.

As the science and technology progresses the Raman instrumentation is planned to be deployed for the first time on the surface of another body in our Solar system. The joint mission of European Space Agency (ESA) and National Aeronautics and Space Administration (NASA) called ExoMars is the future (mission start scheduled to 2016 and 2018) planetary exploration mission to the planet Mars. The main goals for the mission were set thus: to search for signs of past and present life on Mars, to characterise the water/geochemical distribution as a function of depth in the shallow subsurface, to study the surface environment and identify hazards to future human missions, to investigate the planet's subsurface and deep interior to better understand the evolution and habitability of Mars (according to the European Space Agency ExoMars Scientific objectives website http://www.esa.int/SPECIALS/ExoMars/SEM0VIAMS7F_0.html). The main scientific focus of the mission will be on astrobiology and related geological tasks. These tasks will be investigated by several scientific instruments (see <http://exploration.esa.int/science-e/www/object/index.cfm?fobjectid=45103> for the list and description) aboard the rover on the surface and subsurface samples. Among other instruments a Raman spectrometer will be present. This is a major milestone for the Raman spectroscopy and, with a high probability, it is going to be a starting point for the use of Raman spectroscopy in the space missions from that point on. In fact, other planetary exploration missions are going to include Raman spectrometer within a mission payload. Example of such a mission is the NASA/ESA's Titan Saturn System Mission (TSSM) aiming to explore the surface of Titan, Saturn's largest moon and one of the most appealing objects for astrobiologists in our Solar system. Unfortunately, this mission was given a lower priority, in favour of Europa Jupiter System Mission (EJSM) which will focus on studying the sub-surface ocean of Europa.

For full utilisation of Raman spectroscopy on such missions it is necessary to perform as much scientific measurements that will simulate and test the problems and conditions that will be encountered on the missions prior to the start. The Raman spectroscopy works at its best when there is a significant amount of interpreted data related to the studied task available, and the next few pages will review some of the most important applications of the Raman spectroscopy mainly in the field of astrobiology and geology. The Raman instrumentation and the scientific research that takes advantage of it is described in three distinct categories: using the laboratory bench instruments, portable instruments and instruments for a remote acquisition of Raman spectra.

3.1 Portable Raman instrumentation

According to Jehlička et al. (2010a) the portable Raman instruments can be divided into four distinct groups based on their construction characteristics. Instruments specially

constructed by a group of scientists and technicians, usually to perform a specific task. Into this group belongs for example a Deep Ocean Raman In Situ Spectrometer DORISS (based on Kaiser Optics Raman system). The second group consists of Raman instruments capable of collecting spectra from a distance of many meters, examples are Sharma's Raman systems. However, research using this type of instrument will be treated separately in this work, since the remote collection is a quite different scientific approach. Another group of portable Raman systems are small but not so easily movable (primarily due to the weight), due to their dimensions a probe connected by optical fibre cable is frequently used. The highest mobility among the Raman instruments have lightweight handheld instruments operated wholly on batteries, these belong to the fourth group.

A unique Raman system: DORISS: Deep Ocean Raman In Situ Spectrometer was developed for geochemical studies in the deep ocean by Brewer et al. (2004). This heavily modified Raman spectrometer is capable of operation in the depths of 3600 m and at ambient temperature of 1.6 degrees Celsius. For the laser positioning on the opaque mineral samples a positioning system was developed for DORISS by White et al. (2005). Raman spectra of gaseous and liquid CO₂ as well as other materials were reported by Pasteris et al. (2004) as a first step in the investigation of gas hydrates occurring at very high pressures on seafloor zones. This DORISS was able to obtain relevant Raman data on clathrates (hydrates of methane) (Hester et al., 2007) as well as elemental sulphur and bacterial beta carotene in the bacterial mats (White et al., 2006) at seafloor of the Hydrate Ridge at the depths up to 800 m.

Commercially available portable or handheld Raman instruments were developed and originally intended for deployment as in-field detectors for the analysis and the first pass examination of unknown or dangerous chemicals in a forensic context, such as explosives or drugs. Examples of these applications are the detection of drugs of abuse at airports (Hargreaves et al., 2008) and a substantial review of possibilities of commercially available portable Raman instruments for in situ explosives detection (Moore and Scharff, 2009). Several other works using portable Raman instrumentations are now available in the field of forensic science: Harvey et al. (2002) performed a blind field test of unknown substances against a custom hazardous materials reference library with over 97 per cent of samples correctly identified. Edwards and Munshi (2005) used Raman spectroscopy for a forensic detection of biomaterial (illegal trafficking of ivory for instance), Ali et al. (2009) studied the detection of traces of explosives on human nails. A portable Raman integrated tuneable sensor was developed and tested for the detection of hazardous materials such as nerve agents and bacteria spores for homeland security use by Yan and Vo-Dinh (2007), they even manage to detect the trace amounts of these materials using SERS. Portable Raman instrumentation has been also tested and used in the field of arts, Pérez-Alonso et al. (2004, 2006) analysed the degradation products of wall paintings and mortars, Bersani et al. (2006) analysed the medieval manuscripts, Vandenabeele et al. (2007) analysed the museum objects, where the non-destructive approach is crucial. These researches utilise the bigger instruments from the third group with a laser probe.

In contrast, there have been few studies involving the application of portable Raman spectroscopic instruments in other fields, for example, geology. Jehlička et al. (2009a) used a portable instrument to detect common minerals like cerussite, anglesite, wulfenite, titanite, calcite, tremolite, andradite, and quartz under field conditions using the handheld Raman spectrometer First Defender XL from manufacturer Ahura Scientific. They further compared Raman spectra of baryte, almandine, and realgar obtained by this instrument with the data collected with another portable Raman instrument Inspector Raman from manufacturer Delta Nu. The minerals were analysed by the 785 nm excitation laser. Portable Raman instrument proved to be a fast method of distinguishing between different sulphate minerals: gypsum, baryte and anglesite based on the assignments of Raman bands due to the $\nu_1 - \nu_4 \text{SO}_4^{2-}$ vibrations (Jehlička et al., 2009b). The same portable Raman instrumentation was used on the detection of organic minerals whewellite and mellite (crystalline salts of carboxylic acids), aromatic mineral idrialite and samples of amorphous Baltic amber (fossil resin) were recorded in the field and these organic materials are suggested to be added to the list of biomarkers (Jehlička et al., 2009c). Still in the geology field, the portable Raman instrumentation was tested on the assessing of the viability of portable Raman spectroscopy for determining the geological source of obsidian (Kelloway et al., 2010).

The performance of handheld Raman instruments was recently also evaluated in relatively extreme high altitude low temperature conditions on a glacier in Alps. In these researches the First Defender XL from manufacturer Ahura Scientific was employed. Solid forms of pure organic acids (formic, acetic, valeric, hexanoic, heptanoic, isophthalic, ascorbic and mellitic) were measured *in situ* at ambient temperature of -5 degrees Celsius at 2000 metres (Jehlička et al., 2010b) and solid forms of pure nitrogen containing organic compounds were measured *in situ* at ambient temperature of -15 degrees Celsius at 2860 metres (Jehlička and Culka, 2010). All organic compounds were unambiguously detected with rare and acceptably small shifts of measured wavenumbers compared to reference values. The astrobiological implications of these results for example for Titan studies were discussed in Jehlička et al. (2010c). A review of applications of a portable Raman detection of organic compounds at low temperatures and high altitudes with exobiological implications was reported by Jehlička et al., (2010d). The powdered samples of pure organic acids: palmitic, ascorbic, lauric, citric and mellitic acids, the amino acids L-glutamic acid, L-proline, glycine, L-valine, L-alanine and L-leucine as well as D-(+)-trehalose were analysed by Ahura First defender handheld instrument in the five locations under different conditions Jehlička et al., (2010d). First preliminary portable Raman analyses of biomarker and a matrix mineral mixtures as well as biomarkers in a solution were also realised in this study. These type of research has relevancy in the field of astrobiology, especially for future planetary surface exploration missions such as ExoMars, where a miniaturised Raman spectrometer will be called upon to perform data acquisition in hostile environments on the Martian surface and subsurface.

3.2 Remote Raman instrumentation

The remote Raman instrumentation has been developed for a long time now mainly for monitoring purposes in the industrial manufacturing processes. Schoen et al. (1992) used a 100 metres long probe consisting of one excitation and one collection fiber to collect and analyze weak Raman signals of Fe_2O_3 . Skinner et al. (1996) used a Raman microimaging probe using a high-power near-infrared diode for excitation for acquisition of fluorescence-free Raman spectra of high Raman scatterers at distances up to several meters. Sharma et al. (2002a,b) developed a remote telescopic Raman system that was capable of acquiring Raman spectra of various minerals, organic compounds as well as water ice on distances from 10 to 66 metres using a pulsed laser. Stopar et al. (2005) analysed a variety of natural rocks and minerals by a remote Raman system at a distance of 10 metres. They achieved best results with large clear single crystals, while dark fine-grained mineral mixtures produced worse spectra. Sharma et al. (2005) used a portable telescopic system to detect for example gas hydrates and explosives on distances up to 120 metres. Misra et al. (2005) used a pulsed remote Raman system for daytime measurements of mineral spectra for example muscovite ($\text{KAl}_2(\text{Si}_3\text{Al})\text{O}_{10}(\text{OH})_2$) and calcite (CaCO_3). Sharma (2007) reviewed new trends in telescopic remote Raman spectroscopic instrumentation, especially as tools for planetary exploration. Chen et al. (2007) managed to acquire unambiguous Raman spectrum of benzene at a distance of 217 metres using a single 532 nm laser pulse. Sharma et al. (2010) proved a feasibility of application of telescopic Raman instrumentation in the simulated conditions closed to that are currently on the surface of Venus, when they managed to collect Raman spectra of minerals such as talc, olivine, pyroxenes and feldspars under supercritical CO_2 (approx. 95 atm pressure and 423 K) at the distance up to 9 metres.

This type of Raman instrumentation could act in an excellent conjunction with the "standard" Raman instrument for example on the future developed rover for the planetary exploration missions. The remote Raman laser could be used, aside from a camera and radar, as a tool for picking a place of interest from a significant distance and it could save the significant amount of time.

3.3. Applications of Raman spectroscopy for astrobiology related purposes

Raman spectroscopy as an excellent method for studying of minerals was used to closely examine for example interesting hydrated minerals. These are important because the liquid water was required in the geological history to produce them, and the presence of liquid water is one of the basic requirements for a place to host life. Wang et al. (2006) used Raman spectroscopy for a systematic study of magnesium sulphates of various hydration states. The magnesium sulphates are the most common form of sulphates discovered on Mars by the Opportunity rover, along with gypsum and jarosites (Christensen et al., 2004), and their hydration states change depending on the day and night cycle, due to their meta stability weakly bonded structural water molecules. Wang et

al. (2006) found that the crystalline magnesium sulphates can be easily distinguished and that the wavenumber position of the ν_1 sulphate band is shifting towards higher wavenumbers with the decrease in the degree of hydration. Jarosite group minerals were studied by Raman spectroscopy by Sasaki et al. (1998) and the presence of jarosites was confirmed on Mars by Klingelhofer et al. (2004) as an evidence for water based weathering processes. Clay minerals that can also be used as a proofs for weathering involving liquid water were analysed by Raman spectroscopy, in natural samples of montmorillonite the method was able to detect carbon impurities at concentration 0.1 wt% through C-C and C-H bonds (Bishop and Murad, 2004). Sediments from Dry Valleys region in Antarctica (analogous to Martian paleolakes) were analysed by Edwards et al. (2004d). Spectral evidence was found for major differences between oxic and anoxic regions of sediments, and they also found that Raman spectroscopy can be used to reveal traces of biogeochemical processes (sulphate to sulphide metabolism).

Extraterrestrial materials were also analysed using Raman spectroscopy to test the method prior to deploying to on a mission. Rull et al. (2004) analysed Nakha and Vaca Muerta meteorites (achondritic SNC meteorites originating from Mars) using 633 and 785 nm wavelengths and obtained spectra of all major and minor mineralogical components including calcite and aragonite. Another specimen of Martian meteorite was analysed by Wang et al. (2004) with 633 and 532 nm wavelengths and using point-count method when spectra are taken at fixed intervals to reveal the mineralogy. Samples of large ice conglomerates from Earth-space boundary that fell on the surface were analysed by the Raman spectroscopy and compared the data with the isotopic composition of the samples (Rull et al., 2010).

Raman spectroscopy was also used to research at different types of environments that are no less promising from the astrobiological point of view. Raman spectroscopic studies focused on stability of methane clathrate hydrates were performed by Choukroun et al. (2007) with implications to cryovolcanic processes on icy moons of Jupiter and Saturn (most notably Titan). The mineral-microbe interactions in deep-sea hydrothermal systems were studied by Raman spectroscopy in the environment with increased technological difficulty by Breier et al. (2010).

Non-destructive detection of organic minerals that can be found in the geological environment is another field where Raman spectroscopy proves to be irreplaceable. The chemical structure as well as the originating of organic minerals can be quite different. Polycyclic aromatic hydrocarbon mineral idrialite originates as an accumulation of products generated by natural high temperature distillation from specific precursors (Jehlička et al., 2006a). Mellite (Tertiary age, found in lignite and coaly slates), a salt of organic acids originating directly in plant metabolic processes, has been studied using Raman spectroscopy by Jehlička et al. (2006b). Another interesting group of organic minerals originates on self-ignited coal heaps or exposed strata. Examples of these minerals are kladnoite and hoelite which were studied by Jehlička et al. (2007). FT-Raman spectra of fichtelite and hartite (Holocene to Miocene aged pure crystalline terpenes formed from precursor conifer decomposition products) were reported by Jehlička et al.

(2005). These last examples of minerals are genetically close to the fossil resins (typically amorphous mixtures of terpenoids and other chemical substances). Their precursors are the resins of extant or extinct trees with convenient composition and they are formed over the geological timescale buried in the anoxic geological environment. Vibrational spectroscopic methods such as FT-Raman spectroscopy are commonly used as tools for distinguishing between different fossil resins, to shed light on the degree of maturation or authenticity of studied samples (Edwards and Farwell, 1995; Brody et al., 2001). Fossil resins can be found at many localities in the Czech Republic and the usefulness of a non-destructive identification using FT-Raman was demonstrated by Jehlička et al. (2004). To sum it up, organic minerals and fossil resins found in the geological settings are proofs of previous biological activity and can be therefore considered as biomarkers and their Raman spectra should be included into the databases of compounds of interest in the astrobiological studies.

Major importance of Raman spectroscopy as a method for astrobiological exploration of Mars was outlined by Ellery et al. (2004); he proposed both the biomarkers to look for as well as needed Raman instrumentation. In connection with the possible present or past life on Mars, several studies have been performed in the field of detection of protective pigments of extremophile organisms such as bacteria and lichens. Edwards et al. (2004a) used FT-Raman spectroscopy for detection of UV protective pigments β -carotene and parietin in the samples of Antarctic extremophiles and found out, among other things, that Raman spectra of the same species differ depending on the locality and that spectra of relative species are very close. When studying cyanobacterial gypsum halothropic organism Edwards et al. (2005) detected different combinations of pigments chlorophyll, β -carotene and scythenemin in different colonies of organism and established that the best excitation wavelength for this type of studies is 514 nm. Edwards and Jorge-Villar (2010) analysed lichen colonies originating from a volcanic environment and discovered that chlorophyll and carotenoid lutein are ubiquitous and identified other pigments including atranorin, parietin and gyrophoric, pulvinic and usnic acid, great majority of these lichen substances were suggested as important to search for by Edwards et al. (2003), oxalate minerals whewellite and whedellite were detected as well. Desert varnishes from arid areas in Nevada and Colorado have been found to exhibit molecular signatures of β -carotene and scythenemin by FT-Raman spectroscopy by Edwards et al. (2004b). Microbial colonies in halite samples from Atacama desert were studied by Vitek et al. (2010) and the signals from all major pigments and even signals from mycosporine-like amino acids were found, and that the spectral features of the colonisation zones inside one type of habitat differed. Biological modification of iron oxide haematite to goethite (α -FeOOH) was observed by Edwards et al. (2004c). This is an important fact, since iron oxides can act as UV radiation protective substances on Mars surface, where they are abundant in the soil. Goodwin et al. (2006) used Raman microspectroscopy to study halophile *H. salinarium* and discovered that "*carotenoids pigments occur in concentric rings of higher concentration*". Wilson et al. (2007) showed that Surface Enhanced Raman Spectroscopy is capable of detecting a bacterial pigment scythenemin at nM

concentrations extracted from geological samples. Results of previous research provided a background for establishing a Rio Tinto Martian analogue site based on the Raman spectroscopic study of extremophiles (Edwards et al., 2007a)

A Raman spectroscopic study of morphological biosignatures from relict sedimentary fossilised samples acting as analogues to what might be found on Mars was performed by Edwards et al. (2007b) and they found spectroscopic evidence for degradation products of porphyrins and chlorophylls in the samples of Trendall Pilbara stromatolitic cherts. The potential of Raman spectroscopy for the analysis of diagenetically transformed carotenoids was assessed by Marshall and Olcott Marshall (2010) and they found that spectra of diagenetically modified carotenoids can be used as unique diagnostics for the former biological material.

Important studies focused on the **quantitative** aspects of Raman spectroscopy have been carried out recently when analysing experimentally prepared mixtures of biomarkers in mineral matrices. Testing of Raman microspectroscopy for the detection of various different types of biomarkers in feasible mineral matrices (halite, gypsum, epsomite, calcite) is important for it gives the information about the limitations of the method. These types of measurements aim for the evaluation of Raman spectroscopy as a tool for the detection of relatively low concentrations of various biomolecules in mineral environment, trying to simulate the real samples such as microbial colonies in gypsum or halite (endolithic microorganisms). Vitek et al. (2009a,b) used Raman microspectroscopy for identification of beta carotene (a UV protective pigment) in gypsum, halite and epsomite mineral evaporitic matrices directly, as well as measured through crystal of the same mineral. They unambiguously detected concentrations as low as 10 mg.kg^{-1} (0.001wt%). Similarly Osterrothova and Jehlicka (2009) tested the detection of usnic acid (a UV protective pigment, common in lichens) in the same settings. They managed to detect concentrations as low as 1 g.kg^{-1} (0.1wt%) when measured directly and 5 g.kg^{-1} (0.5wt%) when analysed through the crystal. Alajtal et al. (2010) studied the detection of polyaromatic hydrocarbons (PAHs, recognised degradation products of various biomolecules originating in biological processes) such as naphthalene, phenanthrene and triphenylene in quartz, gypsum and calcite mineral matrices and established the detection limits as low as 10 mg.kg^{-1} for naphthalene and 0.25 to 2 mg.kg^{-1} for the other PAHs. The huge differences between the concentrations of molecules that Raman microspectroscopy is able to detect can be explained by the chemical structure of studied molecules. Beta carotene has a long chain of conjugated (-C=C-) bonds and PAHs consist of aromatic rings and both these attributes can trigger Raman resonance effect that in fact amplifies the Raman signal of all bands of such molecules by many orders of magnitude. This can be exploited when detecting very low concentration of molecules in question in the samples.

To conclude this chapter, Raman spectroscopy has been shown to be a versatile method capable of providing interesting and important results in astrobiology and related fields. All the main types of Raman instrumentations, remote, portable and laboratory Raman instruments were tested on the wide spectrum of tasks ranging from the fast detection of minerals and mainly minerals of interest for astrobiology in the natural

settings, analysis of extraterrestrial samples of meteorites, detection and description of various types of organic matter in the geological settings, unambiguous detection of important pigments and other biomarkers in experimentally prepared samples as well as in natural samples of colonies of organisms thriving in the evaporitic minerals.

This work is inspired by the previous research, but it tries to focus solely on tasks involving group of nitrogen containing compounds acting as important biomarkers. The research tasks are modified to obtain deeper understanding for the limitations of the different instrumentations of the method. More complex experimentally prepared samples are studied because it is increasingly difficult to get and interpret valuable data from analysing samples of mixtures of rather similar biomarkers as well as mineral matrices with analogous Raman spectra. Also the portable instruments are much widely used in this work to accommodate to the fact they represent better the instrumentation planned for planetary exploration missions. To test available Raman instrumentation, the outdoor terrain measurements are often performed at locations where the conditions can to some extent simulate the harsh conditions of extraterrestrial planetary surfaces.

4. INSTRUMENTAL AND EXPERIMENTAL

4.1 Laboratory bench Raman spectrometers

The essential instrument used for Raman analyses in this work was a multichannel Renishaw In Via Reflex microspectrometer (Figure 5). Excitation was provided either by the 514.5 nm green line of an argon gas laser with maximum power output 50 mW or by the 785 nm red line of a diode laser which has power output of maximum 300 mW. During the measurements the laser power was never maximised to avoid sample damage. The usual power settings were 5-50% of laser power for both wavelengths. The scanning parameters for each analysis can be adjusted in the wide range of settings. It is possible to choose many parameters such as number of scans, duration of a single scan, precise laser intensity (adjustable step by step increments from very low levels used when handling samples prone to thermal degradation), and selection of any spectral region from the range of 150-4000 cm^{-1} , (which affects the spectral resolution accordingly) to name the most important. Raman spectra were calibrated using the 1332 cm^{-1} line of the diamond and 520.5 cm^{-1} of the silicon standards. The microscope connected to the spectrometer has four objectives providing up to 100 \times magnification. For the majority of analyses a 50 \times objective lens was used, providing a spot diameter of ca. 2 μm . No surface alteration was observed under the conditions used in the measurements. For the under-the-crystal measurements a long focus 50 \times objective was used to gather the Raman signal from the matrix underneath the crystal. Multiple spot analyses on different areas of the same sample provided similar spectra and confirmed the spectral reproducibility.

Samples of minerals were usually measured without any preparation, which is the main advantage of Raman spectroscopy, either by 50 \times objective or by a long focus 50 \times

objective in some specific cases. The experimentally prepared samples of evaporitic matrix mineral containing a selected biomarker of a known concentration were prepared by using a mortar and pestle. Each sample was homogenised for 10 minutes to achieve a good level of immixture. Alternative ways of preparing the samples were tested (ball grinder) but the appearance of new Raman bands in the spectrum (due to agate or solvent) led to reject this approach.

The infrared spectra of minerals were recorded on a Nicolet Magna 760 FTIR spectrometer with 2 cm^{-1} spectral resolution in the $400\text{-}4000\text{ cm}^{-1}$ range). A very small amount of each mineral was used to prepare a mixture with KBr (potassium bromide) and then analysed using the DRIFT method. The resulting spectrum has Kubelka-Munk intensity units.

4.2 Portable Raman spectrometers

Two portable Raman spectrometers were used in this study: namely, a First Defender XL by Ahura Wilmington, MA, USA, and an Inspector Raman by Delta Nu, Laramie, WY, USA. Both instruments are lightweight and utilise the same type of excitation light but they also have significant differences when performing a measurement.

The portable First Defender instrument (Figure 6) weights 1.8 kg and is equipped with a 785 nm diode laser for excitation and a thermoelectrically cooled CCD detector operating at $-50\text{ }^{\circ}\text{C}$. The maximum laser output used in this study is 300 mW at source. This instrument provides Raman data over the wavenumber range $250\text{-}2900\text{ cm}^{-1}$. The effective spectral resolution of this instrument lies in between $7\text{-}10\text{ cm}^{-1}$. This instrument has a built-in display for easier manipulation. Laser power can be set only to "low", "medium" and "high" intensity and the time for collecting the spectrum is set either automatic (spectral acquisition time is determined by the instrument software itself until the satisfactory quality of spectrum is reached) or manual (maximum duration of a scan is 10 seconds).

The portable Inspector Raman instrument (Figure 6) weights 1.9 kg, also uses a 785 nm diode laser at maximum output power of 120 mW and a thermoelectrically cooled CCD detector. It gives Raman data over the wavenumber range $200\text{-}2000\text{ cm}^{-1}$ with a spectral resolution of 8 cm^{-1} . This instrument is controlled remotely via a USB cable connected laptop. It allows the operator to select from a wider range of settings for measurements including more detailed power output selection, number of accumulations and a long accumulation times. The best results were reached when each spectrum was recorded from 10 accumulations each of 5 seconds duration.

Portable instruments were used for Raman analyses under common outdoor conditions as well as to perform analyses at relatively extreme conditions in the winter Alps mountains. Biomarkers were analysed in the form of pure substances, ices of pure substances liquid at room temperature, solutions, mixed with other biomarkers, in the evaporitic matrices and in the evaporitic matrices analysed through the evaporite mineral

crystals. All measurements were carried out in full daylight by shielding the specimen and instrument contact area using a black cloth.

Raman spectra from all instruments were exported into the Galactic .spc format. Spectra were then compared using GRAMS AI (Version 8.0, Thermo Electron Corp, Waltham, MA, USA). Raman spectra were normally not subjected to any data manipulation or processing techniques and are reported generally as collected; in a few cases a commercial baseline correction process was used to extract the data. When analysing the spectra of minerals, the peak fitting Gaussian-Lorentzian function was used to identify the individual bands.



Figure 5 Renishaw In Via Reflex microspectrometer



Figure 6 Portable Raman spectrometers First Defender XL by Ahura (foreground) and Inspector Raman by Delta Nu

5. RESULTS

5.1 Vibrational spectroscopy of nitrogen containing minerals

Boussingaultite and nickelboussingaultite

Secondary sulphate minerals are an interesting and complex group of minerals and vibrational spectroscopy and especially Raman spectroscopy is a great analytical method for distinguishing among often very similar mineral species. For many of the discovered minerals from this group no Raman spectra with appropriate band assignment were published. Boussingaultite, has the chemical formula $(\text{NH}_4)_2\text{Mg}(\text{SO}_4)_2 \cdot 6\text{H}_2\text{O}$ and the sample analysed here originated from Larderello, Tuscany, Italy and has an appearance of yellowish coloured micro crystalline coating. The magnesium atom is surrounded by an octahedron of water molecules, each forming two hydrogen bonds to oxygen atoms of the sulphate ions. Three hydrogen atoms of each ammonium ion are bonded to oxygen atoms in sulphate ions, the fourth hydrogen atom is unique in that it is equidistant from two sulphate-oxygen atoms. In nickelboussingaultite, as its name suggests, Ni^{2+} cations are partially substituted for Mg^{2+} . Its chemical formula is $(\text{NH}_4)_2\text{Ni,Mg}(\text{SO}_4)_2 \cdot 6\text{H}_2\text{O}$. The sample of nickelboussingaultite originated from Cameron, Coconino co., Arizona as a white, finely granular aggregate. Both minerals are not organic minerals in the strict sense, but the ammonia group in the minerals can originate either from geological sources such as fumaroles and geyser localities or from the decaying of organic matter such as anthracite and coal mine dump fires. Unfortunately the vibrational spectroscopy is unable by itself to decide the biological source of the NH_4 group, other methods, such as light isotopes should be used.

The strongest band in the Raman spectrum of boussingaultite at 983 cm^{-1} is attributed to the ν_1 symmetric stretching vibration the SO_4 group, the intensity of this band in the infrared spectrum is quite large, which would suggest that the symmetry of the sulphate groups in the mineral is reduced from tetrahedral. Medium intensity bands at wavenumbers 625 and 615 cm^{-1} and 626 and 616 cm^{-1} are attributed to the ν_4 bending vibration of the SO_4 group. A medium intensity band at 454 cm^{-1} in the Raman spectrum is attributed to the ν_2 bending vibration of the SO_4 group. The broad bands at wavenumbers 787 , 724 , 679 and 566 cm^{-1} can be attributed to the torsion vibrations of water molecules. These bands are absent in the Raman spectrum. The Raman bands at 360 and 310 cm^{-1} could also be attributed to the vibrations of water molecules, while bands appearing at 222 cm^{-1} and below are attributed to the lattice modes. For more detailed information on band assignment see Appendix A.

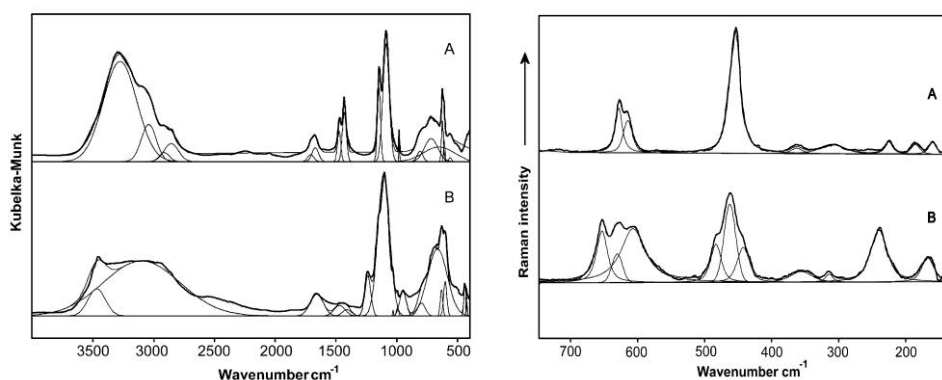


Figure 7 DRIFT spectrum of boussingaultite (A) and nickelboussingaultite (B).
 Figure 8 Raman spectra of the SO_4 bending vibration region (10x magnified);
 boussingaultite (A) nickelboussingaultite (B)

One weak band in the infrared spectrum (992 cm^{-1}) and one strong band in Raman spectrum (990 cm^{-1}) were assigned to the ν_1 symmetric stretching vibration of the SO_4 group. Spectral signatures of the ν_4 bending vibrations of the SO_4 group are stronger in the infrared spectrum, wavenumbers 670 , 620 and 604 cm^{-1} (Figure 7) than in the Raman spectrum 652 , 624 and 602 cm^{-1} (Figure 8). The SO_4 bending ν_2 vibration is given by the bands at 438 and 423 cm^{-1} in the infrared spectrum and bands at 457 and 415 cm^{-1} in the Raman spectrum. The multiplicity of these bands clearly indicates a reduction of symmetry of the sulphate group which is apparently greater than in case of boussingaultite: three bands in bending regions comparing to two bands in spectrum of boussingaultite. These changes as well as the shift in wavelengths of major bands suggest the influence of the nickel atoms that substitute magnesium atoms in the structure of mineral. In addition, the broad bands at wavenumbers ~ 760 , 675 and 520 cm^{-1} can be attributed to the torsion vibrations of water molecules. They can be observed solely in the infrared spectrum. The weak bands at 341 and 312 cm^{-1} can be also attributed to water vibrations and bands at 240 cm^{-1} and bands at lower wavenumbers in Raman spectrum are attributed to the lattice mode. For more detailed information on band assignment see Appendix A.

Observation of multiple bands in the antisymmetric stretching and in the bending regions suggests a lowering in symmetry of the sulphate ions. Of the two minerals, nickelboussingaultite exhibited a greater reduction of symmetry, a possible account for the nickel atoms substitution. It was possible to distinguish between the spectral manifestations of the OH and the NH_4 groups in the stretching and bending regions of the Raman spectra of both minerals, which may be of importance, since life processes and decay of organic matter may be involved in the formation of these minerals.

5.2 Raman spectrometric investigation of biomarkers in evaporitic mineral matrices

5.2.1 Raman microspectrometric investigation of urea in calcite and gypsum powder matrices

The biomarker investigated in this study, urea, was used to demonstrate the possibility of detection of a nitrogen containing common biomolecule, which is chemically and structurally quite different from previously similarly studied biomolecules, e.g. β -carotene and usnic acid. Vitek et al. (2009) managed to detect the β -carotene in mineral matrices at concentration as low as 0.001wt%, while Osterrothova and Jehlicka, (2009) reached the detection limit of usnic acid in mineral matrices at 0.1wt%. Urea is an important compound in astrobiological studies. Urea has been found in extraterrestrial environments together with various amino acids. The gypsum and calcite minerals were chosen for their abundance on Earth as evaporitic minerals. These minerals can serve as substrates for possible microbial life in extreme habitats and both can have either a hydrothermal or an evaporitic origin. Both calcite and gypsum have been found on the planet Mars (Boynton et al., 2009; Langevin et al., 2005).

Samples were prepared at three different concentrations: 25wt%, 5wt% and 1wt%. All detected Raman bands of urea were in excellent agreement (band shift usually 0-1 cm^{-1}) with literature (Keuleers et al., 1999; Frost et al., 2000) The Raman spectra of urea in the calcite (band positions in good agreement with Gunasekaran et al., 2006) matrix at different concentrations are shown Figure 9) for the spectral region between 3600 and 1400 cm^{-1} . Since no Raman bands of calcite are present in the highest wavenumber region the Raman bands of urea cannot be obscured at all. All four Raman bands (3432, 3358, 3322 and 3244 cm^{-1}) can be seen at all concentration levels. The intensities of Raman bands are shown because of the lack of comparison with mineral bands. The intensity is shown to be gradually dropping to as low as 900 units for the concentration of 1 wt%. The lower concentration showed nothing but the noise. In the mid wavenumber region (1800 – 1400 cm^{-1}), as seen in Figure 9, the Raman bands of urea can be found between the two calcite bands at 1750 and 1436 cm^{-1} . All six bands are observed in the spectrum of the highest concentration, even the weakest band at 1680 cm^{-1} , while only two very weak bands are observed at 1649 and 1540 cm^{-1} attributed to the symmetric stretching NH_2 and symmetric stretching CO vibrations, respectively. The strongest Raman band of urea, attributed to the symmetric stretching CN vibration at 1010 cm^{-1} , is located in some distance from the strongest band of calcite at 1086 cm^{-1} , attributed to the symmetric stretching CO_3^{2-} . The lowest spectral region contains only two bands at 712 and 281 cm^{-1} of calcite and one band of urea at 547 cm^{-1} with shoulder at 560 cm^{-1} in the highest concentration of urea. Overall, almost all urea bands have been identified in the calcite matrices.

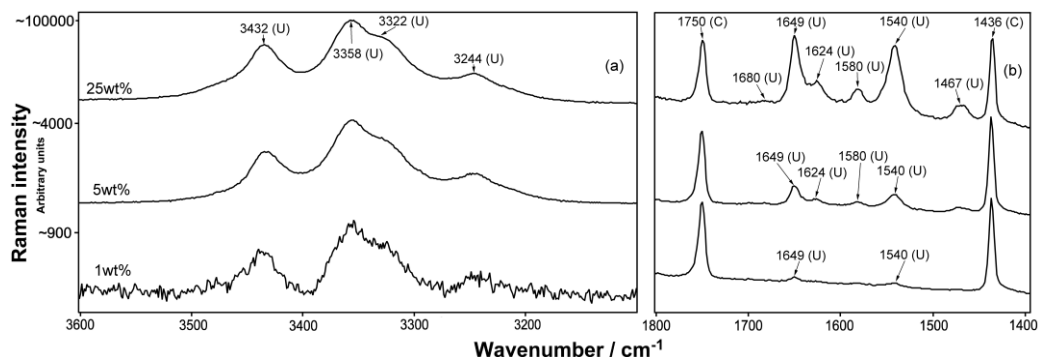


Figure 9 Raman spectrum of urea in calcite matrix in the high wavenumber region; (U) indicates urea band and (C) indicates calcite band

Urea Raman bands acquired from the detection of urea in a calcite matrix through the calcite crystal are shown in Table 2 (Appendix B). It is therefore possible to directly compare this data with the original measurements to demonstrate the loss of urea signal when measured through the monocrystal. The number of detectable Raman bands of urea decreases more rapidly with concentration when measured through the crystal. At a concentration of 1 wt% only two very weak urea bands at 1010 and possibly at 1649 cm^{-1} can be seen. These results suggest that the detection limit of urea in the calcite matrix can be set as 1wt%, while detection limit of urea in the calcite matrix measured through the crystal can be set in the interval between 1 and 5 wt%.

In the case of urea detection in gypsum matrix, gypsum (band positions in good agreement with Kloprogge and Frost, 2000) related Raman bands occupy several spectral regions where Raman bands originating from the urea vibrations are expected. At a concentration of 25 wt% three broad NH_2 stretching vibrational bands of urea (3432, 3322, 3244 cm^{-1}) and two band of gypsum (3495 and 3406 cm^{-1}) have comparable intensities. As the concentration of the urea decreases, the intensity of the urea bands significantly lowers. Therefore only three weak broad bands at 3358, 3322 and 3244 cm^{-1} appear in the 5wt% samples and only one very weak broad band at around 3330 cm^{-1} in the case of 1 wt% sample. All six Raman bands of urea (1680, 1649, 1624, 1580, 1540 and 1467 cm^{-1}) can be detected corresponding to the 25 wt% concentration case, while at the 5 wt% three bands at 1649, 1624 and 1540 cm^{-1} are clearly distinguishable and at 1 wt% concentration only the strongest Raman band of urea (1649 cm^{-1}) can be found in this region. The first part of Figure 10 is given only for the confirmation of the fact that the urea vibrational band at 1010 cm^{-1} does not manifest itself in the spectrum at any concentration level and only the 1008 cm^{-1} gypsum band can be seen. The second part of Figure 10 shows the urea band at 547 cm^{-1} among the observed bands of gypsum. At the highest concentration even the very weak band at 564 cm^{-1} can be observed above the plateau between 550 and 600 cm^{-1} . The intensity of the urea band at 547 cm^{-1} at the 1wt% concentration is so small that a magnified cut out of a picture was used in this case. Overall, the detection of urea is much more difficult in the gypsum matrix than in the calcite matrix. The biggest drawback is the

overlapping of the strongest urea band at 1010 cm^{-1} and the strongest gypsum band at 1008 cm^{-1} .

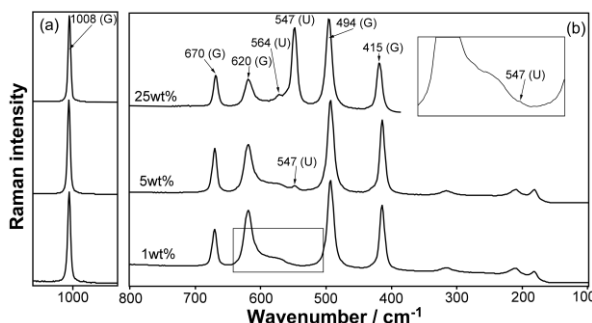


Figure 10 Raman spectrum of urea in gypsum matrix in the low wavenumber region; (U) indicates urea band and (G) indicates gypsum band

The detection of urea in the gypsum matrix through the gypsum crystal appears to be quite difficult. At the concentration of 25 wt% almost all urea bands (with the clear exception of the 1010 cm^{-1} band) can be found in this setting. However, only two weak broad bands at 3322 and 3244 cm^{-1} are detected at the concentration of 5 wt%. At the concentration of 1 wt% no urea Raman bands can be seen in the spectrum. Despite this, the detection limit of urea in the powder gypsum matrix can be set as 1 wt% and the detection limit of urea measured through the gypsum crystal should be definitely set above 5 wt%. For additional figures and tables including the table with all detected urea bands see Appendix B.

This study shows that Raman microspectroscopy can be used for detecting urea, a potential biomarker, in artificially prepared powder mineral matrices. The detection limit of urea both in the calcite and the gypsum mineral matrices, which are contemplated as the possible life supporting environments for example on Mars, is 1wt%. When measured through appropriate transparent crystals, the detection limit of urea in calcite matrix lies in the interval of 1 – 5wt% and for the detection of urea in the gypsum matrix under the crystal the limit is slightly higher than 5wt%.

5.2.2 Raman spectroscopic detection of biomarkers in evaporite matrices and through the transparent gypsum crystal using a portable instrument under Alpine conditions

The aim of this particular research was to utilise Raman spectroscopy in more complex conditions that will be more comparable with real conditions expected in astrobiological research. Until now the potential of portable Raman instruments was tested only on relatively simple tasks namely an evaporite mineral matrix containing a single biomarker compound. The aim of this study was however to test detection of more complex samples under more stringently hostile conditions. The novelty of this research can be summarised as follows: firstly, the studied biomarkers were measured not only as

single compounds (in the mineral matrix) - in the current study mixtures of two or three chemically and structurally similar compounds were measured using a portable instrument in the relatively hostile Alpine environment. The samples of biomarkers in mineral matrices were analysed directly on the surface and also through the natural crystals of gypsum of various thicknesses.

Following pure chemicals acting as biomarkers were used: amino acids glycine and L-alanine, nucleobases thymine and adenine, and metabolite urea. Calcium sulphate dihydrate $\text{CaSO}_4 \cdot 2\text{H}_2\text{O}$ (gypsum) was chosen as a matrix mineral. All chemicals were purchased from Sigma Aldrich. The stated purity of the chemicals was between 98 and 99%. The mixtures of gypsum mineral containing selected biomarkers were prepared using mortar and pestle. One, two and three biomarkers were successively mixed with the gypsum mineral at the total concentration of 50wt%, 10wt% and 1wt%. In a category of urea in gypsum samples at concentration levels of 50wt%, 25wt%, 10wt%, 5wt% and 1wt% were prepared to have a direct comparison with previously published work on similar subject. All the prepared samples were at first measured directly on the surface and then were analysed through a set of transparent, slightly yellowish, natural gypsum crystals. Two crystals (3 mm and 6 mm thick) were used to provide two settings for a laser to pass through the mineral: 3 mm, and 9 mm. A polystyrene calibration standard was used as a reference material for the portable instrument.

Detection of biomarkers in a mixture of five compounds

First preliminary testing trials of a portable instrument used for the detection of biomarkers in evaporitic matrices were conducted inside, in the field laboratory. These qualitative measurements were conducted to ascertain the possibility of the portable instrument used here to identify the Raman bands of complex mixtures of various biomarkers and evaporite mineral matrices. In this phase the mixtures were prepared with equal weight of each compound used. The first sample mixture was prepared from gypsum, epsomite, glycine, L-alanine and mellitic acid and Raman spectrum collected when analyzing this mixture illustrates that only five out of 32 bands due to either biomarker or matrix mineral do overlap (Figure 11). Three biggest intensity bands located at 852 (νCNC), 1018 and 1359 cm^{-1} (CH_3 deformation vibration) are due to L-alanine, bands at 893 (CH_2 wagging vibration) and 1324 (νCCN) symmetric stretching vibration) 601 cm^{-1} are due to glycine. Mellitic acid has fewer medium intensity bands, still, bands at 739 (O-C-OH in plane deformation), shoulder at 377 and 317 (aromatic ring deformation), 236 cm^{-1} can be observed. All wavenumber are in very good agreement with reference values (0-3 cm^{-1}) (Balasubramanian et al., 1962; De Gelder et al., 2007; Jehlička et al., 2006). These results indicate that tested portable Raman instrument is capable to detect all components in the mixture of 5 compounds (three biomarkers and two evaporite minerals).

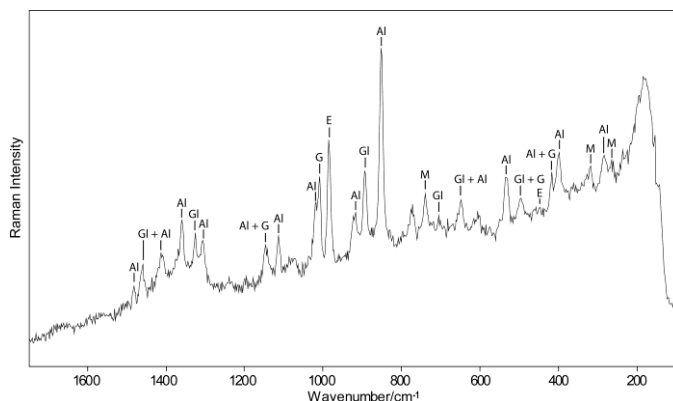


Figure 11 Raman spectra of a mixture of glycine (Gl), L-Alanine (Al), mellitic acid (M), gypsum (G) and epsomite (E). Each component at 20wt% concentration

Detection of biomarkers in a mixture of eight compounds

In the most complex sample eight compounds (of it two evaporite minerals gypsum and epsomite) were mixed together. In this mixture of amino acids, the majority of detected bands has a contribution from two or more detected compounds, either other amino acid or mineral. This is a common issue when detecting single compounds in the mixture of similar compounds. However, from Table 3 (Appendix D) can be seen that the bands due to only a single compound were observed in the spectrum (black marked fields) for five amino acids except L-valine. Glycine and L-alanine have the biggest number of bands that do not overlap with bands of other amino acids. The lower spectral resolution of portable instrument plays increasingly more important role in the complex mixtures as the bands of similar compounds often differ by a few reciprocal centimetres and in the spectrum they usually overlap and the information is partially or completely lost.

Urea in gypsum matrix

Detection of urea in gypsum mineral matrix is hindered by the fact that urea has few medium and strong intensity bands in the lower wavenumbers region and the between 1400 and 1700 cm^{-1} are of medium to weak intensity. Also the strongest urea band ($\nu_1 \text{NCN}$) is located at 1010 cm^{-1} while the strongest gypsum band ($\nu_1 \text{SO}_4$) is located at 1008 cm^{-1} . Urea detection in the gypsum matrix was tested at five different concentrations, for comparison with previous work see Appendix B (Culka and Jehlička, 2010). All observed urea bands are in excellent agreement (typically 0-2 cm^{-1} shift) with references (Keuleers et al., 1999; Frost et al., 2000). Eight bands were observed (1648, 1577, 1540, 1466, 1180, 565, 549 cm^{-1} and a lattice mode band at 180 cm^{-1} plus the ambiguous 1010 band) at 50wt% while only very weak bands at 1180 and medium weak bands at 547 and 180 cm^{-1} when analysed through the 3 mm crystal and weak bands at 547 and 180 cm^{-1} in the case of thicker crystal. In the sample with 25wt% concentration medium intensity bands at 547 and 180 as well as

a weak band at 565 cm^{-1} can be detected. No urea bands were observed when analysed through the crystals. At concentration 10wt% only a weak band at 548 cm^{-1} was detected. Spectra taken at lower concentrations did not contain any Raman bands due to urea both when measured directly and through the gypsum crystals. These results suggest that under experimental conditions tested here, the detection limit of urea in gypsum matrix was at least one order of magnitude worse than in the similar work using the bench instrument (Culka and Jehlička, 2010). Such a high detection limit for the urea in the gypsum matrix can be also explained (apart from the difficult experimental condition and the use of a portable instrument) by the fact that the portable instrument uses the 785 nm excitation laser while the previous work used a 514.5 nm laser, that provided better quality Raman spectra of urea.

Glycine in gypsum matrix

Observed Raman bands of glycine are in excellent agreement (usually 0-3 cm^{-1} shift) with the reference Raman spectrum of glycine (Balasubramanian et al., 1962). In the samples with 50wt% concentration all 12 selected bands (see Table 1) are detected, with slightly lower intensity comparing to the spectrum of pure molecule. The strongest band at 892 cm^{-1} as well as a medium strong band at 1324 is attributed to the combination of NH_3^+ and CH_2 twisting vibration. Band located at 494 cm^{-1} is an overlap of glycine 495 cm^{-1} COO^- bending + CH_2 bending vibration and gypsum 493 cm^{-1} ($\nu_2\text{ SO}_4$) bands so it cannot be taken into account. All weak bands can be observed in this high concentration sample. When measured through the 3 mm crystal all glycine bands are observed with a small decrease of corresponding Raman bands. Big intensity drop of glycine related Raman bands can be seen when measured through the 9 mm crystal (medium intensity band at 893 cm^{-1} and medium weak to very weak bands at 1324, 1115, 1033, 697, 602 and 359 cm^{-1}). As concentration of glycine decreases to 10wt% further reduction in bands intensity can be observed. The strong and medium intensity bands become weak, while other bands become very weak but still distinguishable. Bands at 892 and 1324 cm^{-1} remain the strongest. When measured through the 3 mm crystal only a weak band at 892 cm^{-1} and very weak bands at 1504, 1322, 1032(shoulder) and 357 can be distinguished. When measured through the 9 mm crystal only a very weak band at 894 cm^{-1} and possibly very weak bands at 1504 and 1324 cm^{-1} are detectable. Finally when the concentration of glycine in gypsum drops to 1wt% the distinguishing of glycine bands from the noise in the spectrum becomes impossible. Two features at 892 and 351 cm^{-1} show unconvincing intensity to be considered as bands. The detection limit can be therefore set above the 1wt%. No glycine related Raman bands are observed when 1wt% concentration sample is analysed through gypsum crystals.

Glycine and L-alanine in gypsum matrix

These two amino acids were chosen because they are quite common in natural environment of astrobiological concern are structurally quite similar and are the simplest

of amino acids. Both biomarkers have a great number of Raman bands in addition to the gypsum bands. Reference values are taken from Balasubramanian et al. (1962) for glycine and from De Gelder et al., (2007) for L-alanine and are in a very good agreement. For 50wt% concentration sample all glycine related bands are observed on correct wavenumber position. The alanine contribution to the spectrum consist of 16 bands (of which bands at 1458, 1410, and 1112 cm^{-1} are common to both amino acids) with strongest intensity band of L-alanine located at 851 cm^{-1} : a very strong intensity band at the same wavenumbers in the reference and it is attributed to the (νCNC) stretching vibration. The strong intensity bands due to a CH_3 torsion vibration located at 1357 cm^{-1} in our work and at 1359 cm^{-1} in reference. When measuring through the crystal, in this first sample of two biomarkers, the intensities of Raman bands are quite attenuated. This is presumably a manifestation of the fact that the actual concentration of glycine and L-alanine is only 25wt%. At the concentration of 10wt% of glycine and L-alanine in gypsum only 6 bands due to glycine and 8 bands due to L-alanine can be found in the spectrum with intensities greatly reduced (bands at 1458, 1410, and 1112 cm^{-1} are due to both amino acids). This could be also explained that the exact concentration is actually half for each biomarker. When measured through the 3 mm crystal, five glycine bands can be seen (892 and 695 cm^{-1} are of biggest intensity) and four L-alanine bands (852 cm^{-1} band being the strongest). The same number of Raman bands is detected for each compound when measured through the 9 mm crystal, but the bands are only of very weak intensity. At the concentration of 1wt% only the very weak broad band at 323 cm^{-1} can be attributed to L-alanine and two ambiguous features at 1326 and 853 cm^{-1} are observed. No bands due to any of the amino acids can be observed when 1%wt concentration sample is analysed through gypsum crystals.

Thymine in gypsum matrix

In the next couple of samples the nucleobases thymine and adenine were analysed in the gypsum matrix and through the crystals. All observed Raman bands of thymine are in good agreement (usually 0-4 cm^{-1} shift) with the reference Raman spectrum of thymine (Matlouthi et al., 1984) although the intensities of the bands can differ in some cases. All 11 selected bands can be found in the spectrum taken on the sample of 50wt% concentration of thymine in gypsum. The strong intensity band located at 743 cm^{-1} can be compared to the medium intensity band at 746 cm^{-1} attributed to the $\nu(\text{C}_5\text{-CH}_3)$ vibration. Medium intensity band located at 1368 and very strong intensity band at 1372 cm^{-1} in reference are attributed to the symmetrical $\delta(\text{CH}_3)$ vibration. Spectrum of thymine has numerous Raman bands that hardly ever overlapped by the gypsum matrix band, the band at 617 cm^{-1} is the sole example of overlapping the gypsum band and $\delta(\text{N-C-C})$ thymine band. Spectral resolution of portable instrument allowed to distinguish the relatively closely located bands due to gypsum 415 ($\nu_2 \text{SO}_4$) and 428 cm^{-1} $\delta(\text{C=O})$ of thymine and 493 $\nu_2 \text{SO}_4$ and 479 cm^{-1} $\delta(\text{N-C=C})$ of thymine. These bands appear as double peaks. When measured through the 3 mm crystal all thymine derived bands can be observed (except 1155 cm^{-1} band) with a small decrease in intensity. The situation is similar when measured through the thicker

crystal, ten bands can be observed. While bands at 743 and 1368 cm^{-1} remain the most intense, their relative intensity decreases from strong to medium and from medium strong to medium weak when measured through the 9 mm crystal. As the concentration decreases to 10wt% of thymine in gypsum matrix, only eight bands with respectively lowered intensity can be found in the spectrum (see Table 2 Appendix D). Six of these bands can be detected in the sample spectrum when measured through the 3 mm crystal (1672, 1365, 983, 806, 741 and 482 cm^{-1} , all weak to very weak intensity) and four (1673, 1367, 744 and 429 cm^{-1}) when measured through the 9 mm crystal. In the Raman spectrum of sample with thymine concentration in gypsum of 1wt% the very weak Raman band located at 743 cm^{-1} can be distinguished while two features at 1370 and 986 cm^{-1} are inconclusive. This however suggests that thymine has greater Raman signal response and under these experimental conditions the detection limit of thymine in gypsum can be set slightly above the 1wt%. No thymine derived Raman bands can be distinguished when analysed through the gypsum crystals.

Thymine and adenine in gypsum matrix

Thymine and its nucleobase partner adenine are representatives of important heterocyclic biomolecules, the building blocks of DNA. In the spectrum of 50wt% concentration of thymine and adenine in gypsum sample (see Table 2 and Fig 4 in Appendix D) 11 bands can be attributed to thymine and 14 bands are due to adenine vibrations. The wavenumber positions of adenine Raman bands are in excellent agreement with the reference values taken from De Gelder et al., 2007). The strongest band both in our and reference spectrum is located at 722 respectively at 723 cm^{-1} (reference) and can be attributed to the ring breathing vibration. The number of overlapping biomarker or matrix related bands is greater. Both thymine and adenine contribute to the Raman bands located at 1484, 1369 and 559 cm^{-1} and bands located at 1125 and 620 cm^{-1} are overlaps of biomarker and a gypsum band. When measured through the 3 mm thick crystal the decrease in intensity of biomarker bands is small, but the noise level is increased. All thymine and adenine bands are clearly visible. In the measurement through the 9 mm crystal all but the lowest intensity biomarker bands are visible. All selected bands of both biomarkers can be also seen in the spectrum of sample at 10wt% concentration albeit with lower intensities. When measured through the 3 mm crystal only five Raman bands due to thymine can be observed of which only very weak bands at 988, 804 and 741 cm^{-1} are unambiguous. Nine bands can be distinguished for adenine of which five are unambiguous. When measured through the 9 mm crystal, no Raman bands due to biomarkers could be found. In the spectra taken from the samples with 1wt% concentration of thymine and adenine is possible to distinguish two very weak intensity bands both for thymine (1673 and 984 cm^{-1}) and for adenine (722 and 536 cm^{-1}) so the detection limits can be set to 1wt%. Both compounds appear to have relatively strong response to Raman signal. Such a low intensity bands were not observed when the 1wt% mixture was analysed through the crystals, with the exception of a very weak band 724 cm^{-1} due to adenine.

Portable (handheld) Raman spectrometer was used for the in situ measurements and finally the samples contained complex mixtures of chemically similar compounds to ascertain the ability of the portable instrument to distinguish between them. The analysis of selected biomarkers reported here demonstrated that under these special experimental conditions the portable Raman spectrometer was able to detect the nucleobases thymine and adenine at concentrations of 1wt% in a gypsum host mineral, but it was unable to detect the amino acids glycine and L-alanine at the same concentration. The detection of two similar biomarkers in the gypsum matrix was successful. These results prove that portable Raman spectroscopic instrumentation is capable of detecting biomarkers in more complex samples in a host geological matrix.

For additional data, figures and tables see Appendix D.

5.3 Acquisition of Raman spectra of amino acids outdoors using portable instruments

The aim of this particular study was to collect the Raman spectra of astrobiologically important amino acids using two portable Raman instruments in outdoor conditions. The same set of standards was analysed by two different portable Raman instruments to compare the information obtained from different instruments and appreciate how the resulting data may differ from the data acquired in the laboratory instruments and under laboratory conditions. Solid crystalline forms of selected aliphatic and aromatic amino acids were investigated outdoors at an ambient temperature of 20°C. Pure chemicals, L-Alanine, β -alanine, L-Asparagine, L-Aspartic acid, L-Glutamic acid, L-Glutamine, Glycine, L-Methionine, L-Proline, L-Serine, L-Threonine, L-Tryptophan and L-Tyrosine were purchased from Sigma Aldrich. The stated purity of the chemicals used was between 98 and 99%. A polystyrene calibration standard was used as a reference material for the portable instruments. The two portable instruments used were First Defender XL by Ahura and Inspector Raman by Delta Nu. Technical aspects of used instruments are discussed in the chapter X2. The measurement sessions took place in the courtyard of the building of Geoscience Institutes of the Faculty of Science, Charles University at Albertov (50°04'07'' N, 14°25'27'' E; 200 m) during the daytime and under sunlight. For the measurements with Delta Nu instrument a modified holder of own production was used. The illustration of how the experimental session looked like can be seen Figure 12).

5.3.1 Spectral data comparison between the two instruments

The wavenumber positions of the Raman bands obtained with the portable instruments correspond well with the referenced published Raman data. Usually, the wavenumber difference is better than $\pm(0 - 3) \text{ cm}^{-1}$ and this is critically important for the construction of spectral databases comprising characteristic signatures of biomolecules. The difference of band positions between the two instruments was only $1\text{-}2 \text{ cm}^{-1}$ so their reported band positions are consistent.



Figure 12 Experimental session with Delta Nu operated via laptop computer

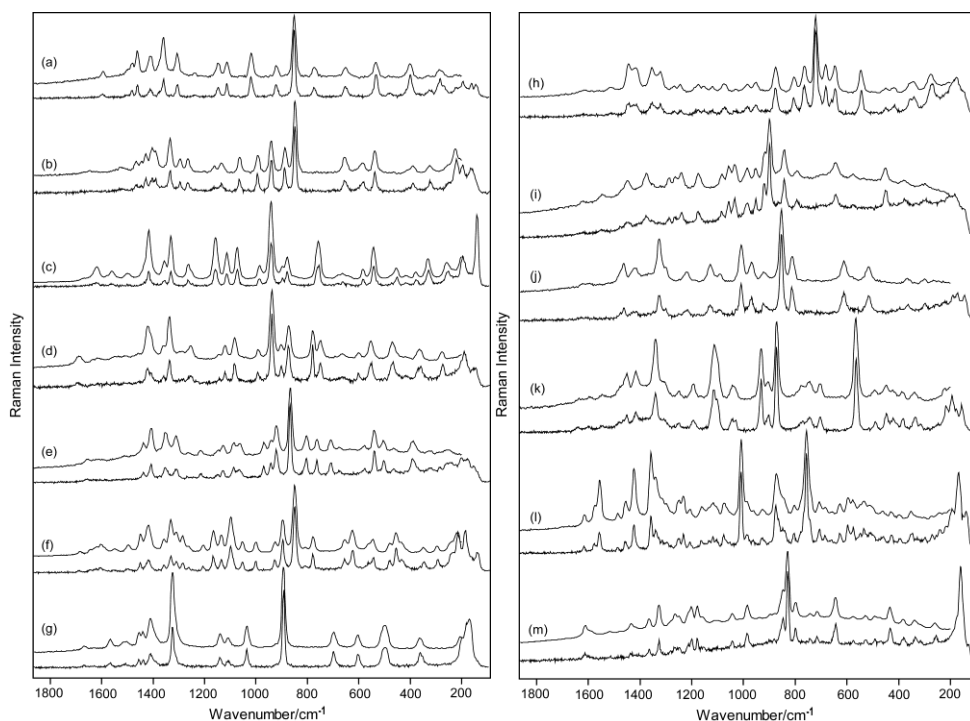


Figure 13 Raman spectra of 13 aminoacids acquired by the Ahura instrument (bottom spectrum in each pair) and Delta-Nu instrument (top spectrum): (a) alanine, (b) β -alanine, (c) asparagine, (d) aspartic acid, (e) glutamic acid, (f) glutamine, (g) glycine, (h) methionine, (i) proline, (j) serine, (k) threonine, (l) tryptophan and tyrosine (m)

The noise level in the spectra of both instruments was quite similar when measured in normal handheld usage. This noise was significantly reduced in measurements utilising a custom made holder for gripping the Delta Nu instrument. The noise is therefore presumably generated mainly from the variations of the laser beam focus when either the instrument or the sample is held manually. These differences are illustrated in the spectra shown in Figure 13. Further reduction of noise level would be achieved by collecting more measurements (Raman spectra) of the same sample and then adding them up in the software. The influence of the fluorescence on the spectra was very similar for the two instruments and can be best observed in the spectrum of proline and tyrosine. Spectra of other amino acids appear to be without a significant fluorescence.

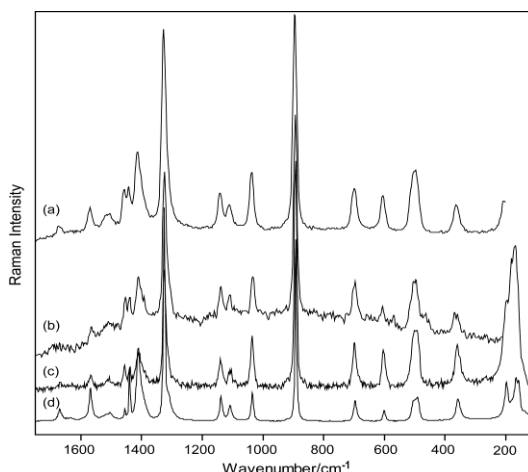


Figure 14 Raman spectra of amino acid glycine acquired by: the Delta-Nu's instrument fixed on a holder (a), without a holder (b), the Ahura's instrument without a holder (c), bench Raman Renishaw instrument (d), no spectral manipulation done

The next important problem to be addressed is the actual spectral resolution adopted in the experimental settings. A FWHM (full width at half maximum) value was chosen for statistical evaluation of the data; FWHM values were taken from the peak fitting procedure in the commercial GRAMS/AI software package. The peak fitting options used were as follows: the fitting function was a specific combination of the Gaussian and Lorentzian function, the selected sensitivity high, and number of iterations was 500. The process was defined on the glycine spectral data. All 15 Raman (see Figure 14) bands of glycine that appear in the spectra of both instruments were added to the data set. The smallest FWHM value for the strongest band was 11.9 cm^{-1} in the case of the Delta Nu instrument and 10.3 cm^{-1} in the case of the Ahura instrument. Some of the weakest Raman bands are quite broad; therefore their respective FWHMs produce outliers in the data set. Instead of simple average a median value was used to resolve this issue and obtain more corresponding results. For the Delta Nu instrument the median value was 18.3 cm^{-1} and for the Ahura instrument, 14.4 cm^{-1} . The same evaluation was made for the glycine spectral

data acquired by a benchtop InVia Reflex Renishaw microRaman instrument. The strongest bands in this case have a bandwidth of 5.5 cm^{-1} and the median value of the FWHM is 12.3 cm^{-1} . These findings are in accordance with the visual appearance of the Raman spectra, while minor changes appear in the spectra taken by Ahura instrument in the spectra taken by Delta Nu instrument (where resolved bands can appear as shoulders), occasionally the closest Raman bands in wavenumber begin to merge together into a compound feature. The possible influence of the laser power level on the bandwidth during the measurements was tested and found insignificant. This indicates that the Delta Nu instrument operates with a slightly worse spectral resolution than the other portable Raman instrument. However, both instruments provide quality results that are comparable with literature defined measurements of Raman wavenumbers.



Figure 15 Ahura scientific employment on the glacier at altitude of 2860 metres

5.3.2 Additional amino acids measurements using Ahura instrument in the Alps

In the conjunction with other portable Raman studies in the high mountain conditions (see chapter 4.2.2), the studied amino acids were measured in the relatively extreme winter Alpine conditions to determine the impact of the surrounding conditions on the quality of the Raman data, especially when compared to the spectra taken on the same compounds with the exactly same instrument. From the results it is apparent that the harsh conditions have only a small influence on the Raman data. For the example spectra of amino acids glycine, proline and tryptophan (see Figure 16). The band positions of the Raman bands are the same when comparing the spectra taken at both locations. The average FWHM values for glycine bands from spectra taken on the glacier were 1 cm^{-1} lower than from the spectra taken at Albertov. The Raman spectra measured on the glacier therefore have slightly narrower bands; this can be due to the lower ambient temperature under the freezing point. However in the spectra of amino acids from the glacier, a small overall increase of the level of noise can be observed (see Figure 16). This fact probably

reflects the influence of the difficult conditions both for the portable instruments and for the human operators.

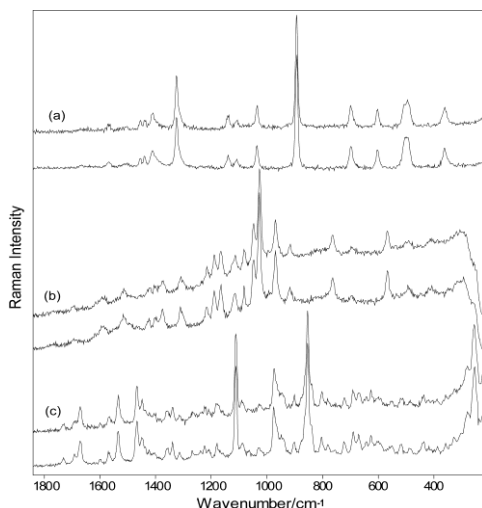


Figure 16 Raman spectra of amino acids glycine (a), proline (b) and tryptophan (c) taken at an altitude of 2860 metres on a glacier (top spectrum in each pair) and at Albertov (bottom spectrum)

5.4 Raman spectroscopic investigation of nitrogen containing organic compounds obtained using a portable instrument under Alpine conditions

This specific task was a part of the first portable Raman instrument measurements in high altitude Alpine conditions and a logical extension to the research involving measurements of pure compounds outdoors. The main goal was to test the performance of commercially available portable Raman instruments in relatively extreme conditions, to assess the quality of output spectral data comparing to reference values. This first research was performed on ices (and solid forms) of pure nitrogen-containing organic compounds. Studied compounds were discovered in tholins (see Chapter 2.3) and are expected to form on such celestial bodies such as on Titan and Triton. The low ambient temperature and the usage of ices at the temperature of dry ice were used to get closer to the actual conditions for example on Titan, although the temperature on the surface of Titan is much lower (94K which is around -180°C). Similar research using the same portable instrument was performed by Jehlička et al. (2010b) on ices of simple organic acids. Solid forms of nitrogen-containing aliphatic and aromatic compounds of representative groups were investigated. Formamide (melting point 2°C), urea (135°C), picoline (3-methylpyridine, -19°C), aniline (-6°C), 1-(2-aminoethyl)piperazine (-19°C) and indoline (-21°C) (for structures see Figure 17) were purchased from Sigma Aldrich. Compounds in glass vials were slowly frozen to -25°C in a freezer. Vials were transported to St Leonhard (1740 m) using a cool box (-80°C), the measurement site was at 2860 m (the Pitztaller glacier, 65 km SW from Innsbruck, Austria, -15°C).

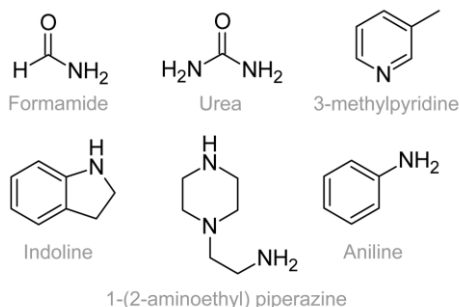


Figure 17 Structures of selected nitrogen containing compounds

Formamide

The NCO stretching vibration band is observed at 1677 cm^{-1} and the NH_2 deformation vibration band is located at 1393 cm^{-1} , both bands are in good agreement with previous Raman observations (Smith and Robinson, 1957). The NH_2 symmetric rocking vibration band can be seen at 1140 cm^{-1} and the CH out-of-plane bending vibration band lies at 1050 cm^{-1} . These bands correspond probably to the bands at 1133 and 1041 cm^{-1} as observed by Itoh and Shimanouchi (1972). The bands at 639 and 615 cm^{-1} can be attributed to the NCO deformation vibration. The strongest broad band located at 208 cm^{-1} is attributed to the lattice vibrations.

Urea

The band located at 1648 cm^{-1} is attributed to the NH_2 symmetric deformation vibration, the band located at 1540 cm^{-1} to the CO symmetric stretching vibration, both bands are in very good agreement with previous observations (Keuleers et al., 1999). The CN antisymmetric stretching vibration band is located at 1466 cm^{-1} ; its symmetric counterpart can be found at 1010 cm^{-1} and represents the strongest band in this spectrum. The NH_2 symmetric rocking vibration band is located at 1176 cm^{-1} . The Raman band at 573 cm^{-1} corresponds to the CO deformation vibration.

3-methylpyridine

The band at 1593 cm^{-1} corresponds to the CH_3 symmetric deformation vibration band, the feature at 1228 cm^{-1} is the C- CH_3 stretching vibration band. The Raman band at 1041 cm^{-1} can be attributed to the CH deformation vibration. Wavenumbers of these medium to strong intensity bands are in a very good agreement with previous laboratory investigations (Gandolfo and Zarembowitch, 1977). Other important bands located at 1190 , 1041 , 801 , 631 and 536 cm^{-1} are clearly observed and attributed to the ring skeletal vibrations.

Indoline

The bands located at 1608 and 1328 cm^{-1} are attributed to the six-membered ring skeletal vibrations. Bands located at 1248 and 1020 cm^{-1} are attributed to the in-plane CH deformation vibrations in the six-membered ring. The band at 1152 cm^{-1} can be attributed to the NH in-plane deformation vibration. The five-membered ring skeletal vibration bands can be found at 880, 778 and 590 cm^{-1} . The out-of-plane deformation vibration bands are located at 860 cm^{-1} (CH) and at 531 cm^{-1} (NH). Proposed assignments are derived from comparison with similar indole molecular Raman features (Lautié et al., 1980).

1-(2-aminoethyl)piperazine

The strong band at 1302 cm^{-1} is attributed to the CN antisymmetric stretching vibration, compared to the band at 1294 cm^{-1} of piperazine investigated by Gunasekaran and Anita (2008). The CC symmetric stretching vibration band is located at 1196 cm^{-1} . The band at 1075 cm^{-1} may be attributed to the CN symmetric stretching vibration. The strong band located at 766 cm^{-1} can be attributed to the CH_2 rocking vibration. The band at 591 cm^{-1} can be attributed to the NH out-of-plane deformation vibration and the band at 450 cm^{-1} may be assigned to the CCN deformation vibration.

Aniline

The medium to strong intensity bands located at 1601, 995 and 818 cm^{-1} are attributed to the ring stretching vibration, ring deformation vibration and ring breathing vibration, respectively, and correspond with the bands at 1601, 995 and 813 cm^{-1} observed on bench instruments by Dollish et al. (1974). The bands at 1029, 757 and 622 cm^{-1} are attributed to the CH deformation vibrations.

All compounds were detected unambiguously using their most intense Raman bands found at their correct wavenumber peak positions, corresponding to previously published values. Excellent reliability and satisfactory spectral resolution (7 – 10 cm^{-1}) was observed for portable instrumentation in the wavenumber range 200 – 2000 cm^{-1} .

6. DISCUSSION

In this chapter, the main results and implications coming from this research work as well as feasibility of the Raman spectroscopy for astrobiological studies in general will be discussed and compared to other related methods such as infrared spectroscopy.

6.1 Raman spectroscopy of nitrogen containing minerals

Two principal methods of vibrational spectroscopic analysis were used for the studies of nitrogen containing minerals: Raman spectroscopy and infrared spectroscopy. The detailed information about instrument used as well as experimental settings are described in the Chapter 4.

The Raman microspectroscopic analysis was used as a method of choice due to several crucial advantages. The samples were analysed without previous preparation of any kind, which was important since several rarer samples were grains as small as of 1 mm in diameter so the first analytical method should have been as much indestructive as possible. The microscope was also a big advantage since it allowed to choose favourable spots on the surface of the sample (such as inside small cavities where the crystals seemed to be better developed and preserved). The laser spot size was circa 3 μm . This micrometric size allowed to take spectra from different parts of a sample, that often appeared slightly different in the microscope to confirm spectral reproducibility. Using the microscope it was possible to locate crystals with different orientation and thus to take spectra where the main crystal plane is oriented directly perpendicular or parallel to the laser beam. The differences between resulting Raman spectra provide unique structural information although they are often hard to interpret. The great range of laser power adjustability was also appreciated since some samples were measured only on few percent of laser power (less than 10 mW). High power outputs sometimes involved unwanted thermal alteration of the sample. Also, the Raman spectra of minerals appear relatively simpler compared to the IR spectra.

As a complementary method to Raman spectroscopy the Infrared spectroscopy provides additional information on the studied sample. However, for the analysis of natural samples of minerals, the Raman spectroscopy seems to be a more preferable method. The crystalline nature of minerals favours the use of Raman spectroscopy especially when Raman spectroscopy with polarised light is employed. Also the possibility of choosing among variety of different excitation lasers can greatly reduce negative effects such as fluorescence in the sample. The frequency and thus energy of excitation is bigger in the case of Raman which allows to significantly lower the energy of the irradiation of the sample and to evade the harmful thermal damage of some materials. Sample preparation is virtually non-existent for Raman analysis, while for example the Diffuse

Reflectance Infrared Fourier Transform Spectroscopy (DRIFT) used in this study involved the powderisation of a mixture of the minerals with KBr (potassium bromide) that is transparent to the infrared radiation. Other less destructive infrared methods such as ATR (Attenuated total reflection) Infrared spectroscopy can be used although they manifest different drawbacks, such as the necessity of the direct contact between the ATR crystal and the sample. The infrared spectroscopy was used as a complementary method to the Raman spectroscopy since in general bands that do not appear in the Raman spectra can be found in the infrared spectra and vice versa (such as $\nu_3(\text{SO}_4)$ vibration that is attributed to the small intensity band in the Raman spectrum while corresponding band in the infrared spectrum has strong intensity). Also, for some functional group with polar bonds, typically NH_4 and H_2O which are important components in the structure of the studied minerals in this work, the deformation vibrations (1675 and 1450 cm^{-1}) as well as corresponding stretching vibrations in the high wavenumbers region ($2800 - 3400\text{ cm}^{-1}$) are manifested both in greater intensity and detail in the infrared spectra. Unfortunately for the DRIFT analysis it was necessary to grind a small amount of each mineral and prepare a mixture with KBr (approximately sample 1:10 KBr) that was then analysed. This means this method is destructive and also that the structural information is lost and an "average" of the sample analysed. The other instrumentation under consideration (ATR) was not used both due to the size and relative softness of the samples. The IR measurements also take considerable longer and attention has to be paid to the energy levels irradiating the samples which are significantly higher for the infrared spectroscopy (hundreds of mW) otherwise the thermal emission artefacts appeared in the spectra as a large very broad bands. During the measuring session was also necessary to calibrate the spectrometer every 10 minutes or so to accommodate for the rising levels of CO_2 and H_2O in the air in the laboratory (from breathing) because the IR spectroscopy is very sensitive to that compounds and it would have impact on the resulting spectra. Despite these drawbacks the data acquired from infrared spectroscopy well complement the Raman data and are often necessary in the process of vibration to band attribution.

Although not focussed on the study of nitrogen containing minerals, the outdoor terrain in-situ measurements of various rock forming minerals using portable Raman instruments provided valuable information about the performance of the instruments. As expected, no major problem were encountered when light-coloured minerals were analysed. Big crystals of quartz, muscovite, albite, calcite and aragonite yielded very good Raman spectra with excellent agreement with the reference spectra. The dark-coloured minerals such as biotite and tourmaline provided no useful Raman spectra mainly due to the excessive fluorescence. The most interesting part was to acquire spectra of relatively small mineral grains in the surrounding matrix using the portable instruments. Accessory minerals such as zircon and apatite as well as almandine (Fe-garnet) with grains sized 0.5 to 2 mm in diameter provided good Raman spectra although the spectral features of surrounding silicate matrix were also quite prominent. The size of a laser spot of portable instruments appears to be crucial for acquiring a Raman spectrum of a single mineral grain within the rock. It is possible that the collecting area of the instruments may be up to a few

millimetres in diameter depending on the focus, which is close to the grain size of the accessory minerals apatite and zircon for example.

To summarise this part: Raman spectroscopy has been previously used to identify and describe nitrogen containing minerals from several groups with examples of chemically and structurally quite diverse minerals. Very good data were published using Raman spectroscopy when analysing nitrogen containing jarosites (Frost et al., 2006b), phosphates (Frost et al., 2005), nitrates (Frost et al., 2004), and organic minerals kladnoite (Jehlička et al., 2007), oxammite (Frost and Weier, 2003), urea (Keuleers et al., 1999). In many of these previous researches the infrared spectroscopy was also used as a complementary method providing additional information about the minerals. In this research work, nitrogen containing minerals such as boussingaultite, nickelboussingaultite, biphosphammite, ammonioborite were investigated using the micro Raman spectroscopy with previously mentioned advantages, with very good quality data as results. Therefore, it is possible to recommend Raman spectroscopy as research method in the fields like geochemistry and astrobiology where detection and analysis of nitrogen containing minerals in the geological rock samples may be very important, for example the porphyrin derived minerals such as abelsonite would provide substantial proof of previous life related biochemical processes, if found in the geological record.

6.2 Raman spectroscopic analysis of nitrogen containing compounds

In this part several approaches in the field of spectroscopic analysis of selected biomarkers and related compounds will be discussed based on the performed research. Experimental tasks include usage of both the laboratory and portable instruments, indoor laboratory and outdoor terrain measurements including relatively extreme conditions, analyses of pure compounds, simple to complex mixtures of various compounds and determination of the detection limits for some compounds.

6.2.1 Analysis of pure compounds

Initially, the selected nitrogen containing compounds were analysed by the Raman microspectrometer in the laboratory. Among the studied compounds were amino acids, nucleobases, and metabolites such as urea and uric acid. This data were collected mainly for the purposes of comparison with the data acquired by the portable instruments. As expected the spectra of pure compounds collected by the microspectrometer in the laboratory were in excellent agreement with the previously published references and featured narrow Raman bands and virtually no background noise.

The next step was to perform the outdoor measurements using the portable instrumentation on the same pure nitrogen containing compounds. The purpose for the testing of the two different types of the portable Raman instruments was and to learn the quality of the resulting Raman data, to directly compare the data from the instruments, to confront the resulting data with the spectra acquired using the laboratory Raman

instrument and other reference values, and as well as to learn how to operate the instruments efficiently. Spectra of thirteen amino acids (for full list see Appendix C) were collected using both the Ahura and Delta Nu portable Raman instruments outdoor, under sunny weather conditions. The amino acid were selected because of their importance in the field of astrobiology as well as for their relatively complex Raman spectra, containing many bands, some of them closely located as well as doublets and shoulders.

Raman spectra obtained from the portable instruments were of very good quality typically with 0-3 cm^{-1} difference from references and 1-2 cm^{-1} among the two instruments. Moderately low level of noise was present in the spectra, using the improvised holder the level of noise significantly lowered, noise is presumed to be generated mainly from the variations of the laser beam focus when instrument is hand held. Noticeable fluorescence was observed only in the spectra of proline and tyrosine. The spectral resolution was measured using parameter FWHM (full width at half maximum). Widths of bands was noticeably larger in the Raman spectra from portable instruments. Statistical analysis on the glycine data showed, that the smallest FWHM value for the strongest band (due to νCCN stretching vibration) was 11.9 cm^{-1} in the case of the DeltaNu instrument and 10.3 cm^{-1} in the case of the Ahura instrument, compared to the 5.5 cm^{-1} . Corresponding median values (18.3 cm^{-1} Delta Nu, 14.4 cm^{-1} and 12.3 cm^{-1}) for all the glycine bands suggest that the Delta Nu operates with lower spectral resolution and while this is generally not a problem, in some cases the shoulders disappear and the doublets appear as one broad band.

The overall quality of spectra acquired by the portable spectrometers can be attributed to the fact that these types of instruments were designed to analyse unknown "white powders" in the first place. Fast detection and relative simple operation during the measurements indicated that these small and lightweight portable instruments even in their current (tested) state provide us powerful tools that the next generations shall be used in the planetary exploration missions. Certainly, pure biomarker compounds cannot be expected to be found for example on Mars. Therefore, in the next paragraphs the results coming from analyses of the more complex samples, more resembling the natural samples, are going to be discussed.

6.2.2 Analysis of compounds in the mixture

To test the ability of a Raman spectroscopy to distinguish among the different compounds in a matrix/biomarker mixture is important since the natural samples are often more complex. The fact, that the more different compounds in the sample, the more Raman bands appear in the spectrum suggests, that the overlapping of the bands starts to be an issue, even more in the case of portable instruments with their higher bandwidths. The situation is further complicated when the studied compounds are chemically close (such as different amino acids) since the same functional group of the molecules not so different, give rise to bands located at wavelengths close together or even at the same

positions. The experiments, where at least two evaporitic minerals and at least three biomarker compounds were mixed together, were performed to simulate natural samples.

The experimental mixtures were prepared with each compound having a weight concentration of $(1/n) \times 100$ wt%. This relatively high concentrations enabled the good signal output for the qualitative analysis. The mixture of five compounds, two matrix minerals (gypsum and epsomite) and three biomarkers (glycine, alanine and mellitic acid) was analysed using portable Ahura instrument and from the resulting spectra can be observed that all the main bands are present for each compound with minimum overlapping. At least three unambiguous bands for biomarkers and two for the mineral matrix minerals are sufficient enough to distinguish between the compounds. The more complex sample was then analysed using the same settings and instrument. The total of eight compounds (gypsum, epsomite, glycine, alanine, proline, valine, leucine and glutamic acid) each at 12.5 wt% concentration provided a very complex spectrum with many bands that overlap because the amino acids are chemically very close. As can be seen from the Table 3 in Appendix 4, almost each detected Raman band exhibited the vibrational contribution of two or more amino acids or the matrix mineral (sometimes as much as five). From the same table can be read that at least one Raman band belonging solely to one amino acid was observed for five out of six amino acids (all except valine). This is certainly not sufficient to distinguish each individual compound but serves as a proof that in mixtures of a larger number of similar compounds it becomes extremely difficult or impossible to distinguish (detect) each compound, even when the concentrations are quite high.

These results imply, that the tested portable Raman spectrometers are capable to detect and distinguish individual compounds, both the mineral and the biomarker components of the samples. Of course, in the natural environment even more complex samples can be found in the geological environment, but these first steps showed that even portable instruments provided relatively good results in the analyses of mixtures, and with additional necessary improvements such as better spectral resolution (narrower bands) even more components in the samples should be detectable. The research involving the testing the ability of Raman spectroscopy to detect low concentrations of selected biomarkers will be discussed in the following paragraphs.

6.2.3 Detection of low concentrations biomarkers in the mineral matrix

Probably the most interesting objective is to determine the lowest possible concentrations of different selected biomarkers and different matrix minerals using different Raman instrumentation. This type of research has a major significance in the field of astrobiology since the biomarker molecules are expected to be found at low concentration (if any) and various biomarkers can be detected at diametrically different concentrations. This work involved analyses of the model experimentally prepared mixtures of various concentrations of biomarkers dispersed in matrix consisting of the evaporitic minerals, in order to try to simulate the real conditions where the organisms that produced the biomarkers lived. The samples containing low concentrations of

biomarkers in mineral matrices were analysed both by the laboratory Raman microspectrometers and the portable instruments outdoors, to see if either type of instrument is better suited for this type of measurements. The actual detection limits for nitrogen containing compounds in the evaporitic matrix determined in this work turned out to be quite high (the lowest reached concentrations were relatively high), compared to similar works. For example the detection limit for urea in gypsum matrix using laboratory instrument was 1 wt% (10 wt% using the portable instrument under unfavourable experimental conditions). This can be attributed to the low sensitivity of Raman spectroscopy to the smaller molecules with many functional groups such as NH_2 and OH in the amino acids and urea. With similar experimental conditions, Raman spectroscopy provides better results when detecting molecules with significant skeletal structure such as including one or more aromatic rings. Osterrothová and Jehlička (2009) detected usnic acid in gypsum at concentration of 0.1 wt%, Alajtal et al. (2010) managed to detect naphthalene in the gypsum matrix at concentration of 0.001 wt%. A special structural feature, a conjugated double bond of beta carotene, that enables the signal enhancement by resonance effect, allowed Vitek et al. (2009) to detect this pigment in gypsum matrix at concentrations as low as 0.001 - 0.0001 wt% depending on the wavelength used. In the measurements that were conducted using the portable Raman instrument under the Alpine winter condition, the detection limits were approximately one order of magnitude higher than when analysing the same sample in the laboratory using the bench instrument. Using the Ahura portable Raman spectrometer the detection limit of biomarkers in gypsum was determined at 10 wt% for urea, 5 wt% for amino acids glycine and alanine, and 1 wt% for nucleobases adenine and thymine that contain aromatic structures in their molecules.

The approach used in this part of the research, that is, a powdered compound A dispersed in powdered compound B demonstrated some typical characteristics that need to be discussed more in the following paragraphs.

Sample inhomogeneity versus the laser spot size

When using mortar and pestle for the sample preparation the largest issue is a sample inhomogeneity on the microscopic level. The grain size is usually comparable or bigger (typically averaging 10 μm) than the diameter of the laser spot (<5 μm). Further reduction in size is possible for example when using a ball mill. This was also tested, but since the necessity of using a fluid medium, some additional features of uncertain origin were observed in the resulting Raman spectra, and this approach was rejected. Sample inhomogeneity is generally not a problem, when analyses are performed using portable instruments. It is difficult to determine the exact size of a laser spot in this case, but typical diameter can be between 0.5 to 1 mm depending on the focus and other conditions. These substantially larger areas of signal collection seem better suited to provide an accurate average sample composition.

Colour of the sample components

The degree of sample inhomogeneity can be best observed when analysing coloured compounds such as beta-carotene where the selection of a spot for analysis can be difficult in order to represent the "average" sample. This was not the case when analysing nitrogen containing compounds in evaporitic minerals since nearly all of them are white coloured. Nevertheless, the analyses were performed typically on 3 - 5 different spots of the sample, and when observable differences in the spectra occurred, the average spectrum was created. For some tests the evaporitic minerals were replaced by the Martian regolith simulant, but when analysed using the portable instruments, the analysed spot was burnt out, even on the lowest energy settings. This is attributed to both the brown-red colour that absorbs the laser radiation as well as the particle size.

Differences between matrix minerals

All minerals used in this part of study are transparent when used in the form of large natural crystals (that was used for under-the-crystal measurements) and become white powders when ground. In general, the detection of biomarkers in sulphate mineral matrix is more difficult (comparing to halite for example) due to the fact that gypsum and epsomite have up to eight Raman bands in the low wavenumber region while halite has no Raman bands. This is due to the fact that no vibrational mode in the halite mineral (NaCl) is Raman active. In the natural halite crystals sometimes a slight fluorescence from impurities or other features such as irregularities and cracks in the crystal can have a negative impact on the Raman spectrum but they have much smaller significance than the proper matrix Raman bands. Gypsum bands sometimes coincide (plus minus few reciprocal centimetres which is under the resolution limit of portable instruments) with biomarker related bands and thus make their detection harder. The best results were achieved when using the matrix of the mineral calcite.

Detection limit of a compound in the matrix

At the low concentration, the Raman signal of the dispersed biomarkers rapidly decreases, while the signal of the surrounding matrix remains almost the same until. Ultimately, the Raman signal (bands) of the biomarker is no longer distinguishable from the surrounding noise. The detection limit of a molecule is usually set when its Raman bands have at least two times the intensity of surrounding noise. In this work the band intensities were used, although the band surface can be also used. However, several difficulties appear when trying to determine the detection limits for different biomarkers, such as big differences between the Raman bands of the same compound. For example, in the Raman spectrum of urea, the most intense Raman band (1010 cm^{-1} NCN stretch) has approximately three times the intensity of the second strongest band (547 cm^{-1} NCN bend) and about 10 times the intensity of the third most intense band. This complicates the evaluation of the spectra, since the weak bands can be nearing their detection limits while

the strongest band has still a significant intensity. This is unfavourable since the single band should not be used in most situation for the identification of a compound, preferably at least three different bands should be observed. Fortunately, the amino acids and nucleobases have many Raman bands of comparable intensities, although one strongest band is prominent in the majority of the studied compounds.

Another problem arises when the biomarker and a matrix mineral have important bands located at the same (or very close) wavenumber position. This is again the case of urea dispersed in the gypsum matrix: the strongest urea Raman band (1010 cm^{-1} NCN stretch) overlaps with 1008 cm^{-1} SO_4 stretch and therefore, other bands of significantly lower intensities have to be used. This problem is matrix related and Raman spectra of mixtures of urea with other minerals such as calcite or epsomite do not exhibit such an overlap and some minerals even have no Raman bands at all (halite).

Detection of biomarkers through the transparent crystals

The analyses of biomarkers through the natural crystals of transparent minerals are performed to assess the potential of Raman spectroscopy to obtain spectra from biomarkers located under/inside the sample mineral, the fact that simulates the occurrence of microbial colonies that shield themselves from the UV radiation. Both laboratory Raman microspectrometer and portable instrument were tested. In the case of a Raman microspectrometer the confocal mode of analysis allowed to effectively focus beneath the 1.5 mm thick crystals of calcite and gypsum when detecting urea in mineral matrix. When measured through the crystals, the Raman microspectroscopy was able to detect the concentration about 5 times greater than in regular measurements (5 wt% instead 1 wt%), but no special problems were encountered.

Portable instrument Ahura was also similarly tested in the Alpine conditions. The portable instrument lacks the ability of focussing through the crystal, but features the much wider laser spot and large energy of the laser to compensate the signal loss during the transit of the radiation through the crystal. In these measurements quite thick crystals were used (3 and 9 mm thick crystal of natural gypsum mineral). Wide range of biomarker concentrations were tested as well (from 50 wt% to 1 wt%). Analyses of 50 wt% concentrations of biomarkers through the thick 9 mm crystal confirmed that all important Raman bands of biomarkers are detected, albeit with a great decrease in intensity. At the lower concentrations the nucleobase thymine was detected using several bands at concentration of 10 wt% through the 9 mm crystal while only one very weak band (894 cm^{-1}) was observed for glycine. No reliable Raman bands were found when detecting the biomarkers through the crystal at concentration of 1 wt%. When compared to the original measurements without the covering crystal (only adenine and thymine were detected at concentration of 1 wt%) these results suggest that the crystal presence and its thickness has less influence on the resulting detection of biomarkers and that the decrease in concentration is the main agent when detecting a compound in the matrix.

From the results and findings in this work as well as from the references, it can be concluded that the Raman spectroscopy can be used to detect small concentrations of biomarkers in experimentally prepared mineral matrices. Also for each compound the exact concentration that can unambiguously detected can be very different (even in orders of magnitude). For the studied nitrogen containing compounds, however, the detected concentration were quite high. This can be explained by the fact that these biomarkers have relatively small and structurally simple molecules with small Raman cross sections, unlike for example the carotenoid pigments or polyaromatic compounds.

6.2.4 Measurements in relatively extreme Alpine conditions

The portable instruments were repeatedly tested in several experimental tasks in relatively hostile conditions in order to determine their serviceability and the quality of acquired Raman data. Results of these tests are significant because the future planetary exploration missions will take place in a quite hostile environments, such as a planet Mars or Titan, the moon of Saturn. In this research the ices of several nitrogen containing molecules and structurally similar molecules without nitrogen were analysed by portable Raman instrument Ahura in the Alpine winter conditions to assess the quality of the resulting data. The selected compounds as well as experimental conditions were chosen to partially simulate the conditions and chemistry on the Titan, Saturn's largest moon. The studied compounds (formamide, urea, 3-methylpyridine, aniline, indene, 1-(2-aminoethyl)piperazine, indoline and benzofuran) were chosen because they were found in simulated Titan tholins and some of them are important for life. Except urea, they were all analysed in the form of ice at about -80°C temperature (compared to about -180°C on the surface of Mars). The studied compounds were deeply frozen using the solid CO₂ which helped to decrease the degree of sample melting as encountered by Jehlička et al. (2010b). This study confirmed that the portable instrument tested is able to obtain and unambiguously detect the nitrogen containing compounds in the form of ices with a very good agreement with reference values (0-3 cm⁻¹ difference) and satisfactory spectral resolution (7-10 cm⁻¹).

In addition to this research involving the analysis of pure compounds in the form of ice, some other tasks described above were investigated. The detection of low concentrations of biomarkers in evaporite mineral matrices as well as the similar samples measured through the crystals of gypsum and calcite was performed also in the Alpine conditions. The overall quality of resulting data and the with which the instruments operated in these difficult conditions are quite promising, considering that the future planetary exploration missions with the astrobiological focus are to take place on the surface of the bodies in the larger distance of the Sun.

7. GENERAL CONCLUSIONS

Raman spectroscopy was applied in the study of selected nitrogen containing compounds, that are important in the astrobiological context, to determine the strong points as well as the limitations of the method in several applications, in the prospect of the future use of the Raman spectroscopy as an advantageous method for the future planetary exploration missions with astrobiological context.

In the case of the nitrogen containing minerals, the indestructive analysis, small laser spot and a possibility of selecting the suitable excitation source allowed to obtain good quality spectra of minerals often with miniature grain sizes on the samples. For some of these minerals the band assignment was performed and published for the first time.

Complex mixtures of three biomarkers and two evaporitic minerals were analysed with a portable instrument, and all compounds were unambiguously detected. In the samples containing more of the similar compounds with many bands such as amino acids, the portable instrument was able to detect and distinguish up to five compounds.

Lowest possible detected concentrations of selected biomarkers in the evaporitic minerals were determined when analysed both by micro Raman and portable instrumentation. The exact values of concentrations for the nitrogen containing compounds were generally quite high, in the contrast to the carotenoid compounds. The lowest concentration detected was for the aromatic heterocyclic nucleobases in the gypsum matrix: 0.1 wt%. In this research the laser spot size had the great effect.

Portable instruments were tested in the difficult Alpine winter conditions and provided good quality spectra corresponding with the reference values for samples including pure solid compounds, ices of nitrogen containing compounds, minerals and biomarker-mineral mixtures.

Raman spectroscopy proved to be a feasible method tested in several research scenarios, although it is apparent that besides for example the different excitation wavelength other variables such as laser spot size can significantly change the output of an experiment, and that the interpretation of the results in relation to the planned missions and proposed experiments must be given the utmost attention.

8. REFERENCES

- Alajtal A. I., Edwards H. G. M. and Scowen I. J. (2010): Raman spectroscopic analysis of minerals and organic molecules of relevance to astrobiology. *Anal. Bioanal. Chem.* 397 215–221.
- Ali E. M. A., Edwards H. G. M., Hargreaves M. D. and Scowen I. J. (2009): Detection of explosives on human nail using confocal Raman microscopy. *J. Raman Spectrosc.* 40 144–149.
- Altaner S. P., Fitzpatrick J. J., Krohn M. D., Bethke P. M., Hayba D. O., Goss J. A. and Brown Z. A. (1988): Ammonium in alunites. *Am. Miner.* 73 145–152.
- Alvi K. A., Tenenbaum L. and Crews P. (1991): Anthelmintic Polyfunctional Nitrogen-Containing Terpenoids from Marine Sponges. *J. Nat. Prod.* 54 71–78.
- Andrut M., Harlov D. E. and Najorka J. (2004): Characterization of ammonioleucite $(\text{NH}_4)[\text{AlSi}_2\text{O}_6]$ and ND_4 -ammonioleucite $(\text{ND}_4)[\text{AlSi}_2\text{O}_6]$ using IR spectroscopy and Rietveld refinement of XRD spectra. *Mineral. Mag.* 68 177–189.
- Artemieva N. and Lunine J. I. (2005): Impact cratering on Titan - II. Global melt, escaping ejecta, and aqueous alteration of surface organics. *Icarus* 175 522–533.
- Artemieva N. and Lunine J.I. (2003): Cratering on Titan: impact melt, ejecta, and the fate of surface organics, *Icarus* 164 471–480.
- Atreya S. K., Adams E. Y., Niemann H. B., Demick-Montelara J. E., Owen T. C., Fulchignoni M., Ferri F. and Wilson E. H. (2006): Titan's methane cycle. *Planet. Space Sci.* 54 1177–1187.
- Balasubramanian K., Krishnan R. S. and Iitaka Y. (1962): Raman Spectrum of Gamma Glycine. *Bull. Chem. Soc. Jpn.* 35 1303–1305.
- Barker D. S. (1964): Ammonium in alkali feldspars. *Am. Mineral.* 49 850–858.
- Barks H. L., Buckley R., Grieves G. A., Di Mauro E., Hud N. V. and Orlando T. M. (2010): Guanine, Adenine, and Hypoxanthine Production in UV-Irradiated Formamide Solutions: Relaxation of the Requirements for Prebiotic Purine Nucleobase Formation. *ChemBioChem* 11 1240–1243.
- Bernstein M. P., Sandford S. A., Allamandola L. J. and Chang S. (1995): Organic Compounds Produced by Photolysis of Realistic Interstellar and Cometary Ice Analogs Containing Methanol. *Astrophys. J.* 454 327–344.
- Bernstein M. P., Dworkin J. P., Sandford S. A., Cooper G. W. and Allamandola L. J. (2002): Racemic amino acids from the ultraviolet photolysis of interstellar ice analogues. *Nature* 416 401–403.
- Bersani D., Lottici P. P., Vignali F. and Zanichelli G. (2006): A study of medieval illuminated manuscripts by means of portable Raman equipments. *J. Raman Spectrosc.* 37 1012–1018.
- Bishop J. L. and Murad E. (2004): Characterization of minerals and biogeochemical markers on Mars: A Raman and IR spectroscopic study of montmorillonite. *J. Raman Spectrosc.* 35 480–486.

Botta O., Glavin D. P., Kminek G. and Bada J. L. (2002): Relative amino acid concentrations as a signature for parent body processes of carbonaceous chondrites. *Origins Life Evol. Biosphere* 32 143–163.

Boynton W. V., Ming D. W., Kounaves S. P., Young S. M. M., Arvidson R. E., Hecht M. H., Hoffman J., Niles P. B., Hamara D. K., Quinn R. C., Smith P. H., Sutter B., Catling D. C. and Morris R. V. (2009): Evidence for Calcium Carbonate at the Mars Phoenix Landing Site. *Science* 325 61–64.

Breier J. A., White S. N. and German C. R. (2010): Mineral–microbe interactions in deep-sea hydrothermal systems: a challenge for Raman spectroscopy. *Phil. Trans. R. Soc. A* 368 3067–3086.

Brewer P. G., Malby G., Pasteris J. D., White S. N., Peltzer E. T., Wopenka B., Freeman J. and Brown M. O. (2004): Development of a laser Raman spectrometer for deep-ocean science. *Deep Sea Res. Part I*

Briggs R., Ertem G., Ferris J. P., Greenberg J. M., McCain P. J., Mendoza-Gomez C. X. and Schutte W. (1992): Comet Halley as an aggregate of interstellar dust and further evidence for the photochemical formation of organics in the interstellar medium. *Origins Life Evol. Biosphere* 22 287–307.

Broadfoot A. L., Atreya S. K., Bertaux J. L., Blamont J. E., Dessler A. J., Donahue T. M., Forrester W. T., Hall D. T., Herbert F., Holberg J. B., Hunter D. M., Krasnopolsky V. A., Linick S., Lunine J. I., McConnell J. C., Moos H. W., Sandel B. R., Schneider N. M., Shemansky D. E., Smith G. R., Strobel D. F. and Yelle R. V. (1989): Ultraviolet Spectrometer Observations of Neptune and Triton. *Science* 246 1459–1466.

Brocchieri L. and Karlin S. (2005): Protein length in eukaryotic and prokaryotic proteomes. *Nucleic Acids Res.* 33 3390–3400.

Brody R. H., Edwards H. G. M. and Pollard A. M. (2001): A study of amber and copal samples using FT-Raman spectroscopy. *Spectrochimica Acta Part A: Molecular and Biomolecular Spectroscopy* 57 1325–1338.

Chen T., Madey J. M. J., Price F. M., Sharma S. K. and Lienert B. (2007): Remote Raman spectra of benzene obtained from 217 meters using a single 532 nm laser pulse. *Appl. Spectrosc.* 61 624–629.

Choukroun M., Morizet Y. and Grasset O. (2007): Raman study of methane clathrate hydrates under pressure: new evidence for the metastability of structure II. *J. Raman Spectrosc.* 38 440–451.

Christensen P. R., Wyatt M. B., Glotch T. D., Rogers A. D., Anwar S., Arvidson R. E., Bandfield J. L., Blaney D. L., Budney C., Calvin W. M., Fallacaro A., Fergason R. L., Gorelick N., Graff T. G., Hamilton V. E., Hayes A. G., Johnson J. R., Knudson A. T., McSween Jr. H. Y., Mehall G. L., Mehall L. K., Moersch J. E., Morris R. V., Smith M. D., Squyres S. W., Ruff S. W. and Wolff M. J. (2004): Mineralogy at Meridiani Planum from the Mini-TES Experiment on the Opportunity Rover. *Science* 306 1733–1739.

Clark J. R. and Christ C. L. (1959): Studies of borate minerals. (VII); X-ray studies of Ammonioborite, larderellite and the Potassium and ammonium pentaborate tetrahydrates. *Am. Mineral.* 44 1150–1158.

Croswell K. (1996): *Alchemy of the Heavens*. Anchor. ISBN 0-385-47214-5.

- Culka A. and Jehlička J. (2010): Raman microspectrometric investigation of urea in calcite and gypsum powder matrices. *J. Raman Spectrosc.* 41 1743–1747.
- De Gelder J., De Gussem K., Vandenabeele P and Moens L. (2007): Reference database of Raman spectra of biological molecules. *J. Raman Spectrosc.* 38 1133–1147.
- Dill H. G. (2001): The geology of aluminium phosphates and sulphates of the alunite group minerals: a review. *Earth Sci. Rev.* 53 35–93.
- Dollish F. R., Fateley W. G. and F. B. Bentley (1974): *Characteristic Raman Frequencies of Organic Compounds*. Wiley, New York.
- Edwards H. G. M. and Farwell D. W. (1995): Fourier transform Raman spectroscopy of amber. *Spectrochim. Acta, Part A* 52 1119–1125.
- Edwards H. G. M., Newton E. M. and Wynn-Williams D. D. (2003): Molecular structural studies of lichen substances II: atranorin, gyrophoric acid, fumarprotocetraric acid, rhizocarpic acid, calycin, pulvinic dilactone and usnic acid. *J. Mol. Struct.* 651 27–37.
- Edwards H. G. M., Cockell C. S., Newton E. M. and Wynn-Williams D. D. (2004a): Protective pigmentation in UVB-screened Antarctic lichens studied by Fourier transform Raman spectroscopy: an extremophile bioresponse to radiation stress. *J. Raman Spectrosc.* 35 463–469.
- Edwards H. G. M., Moody C. A., Jorge-Villar S. E. and Mancinelli R. (2004b): Raman spectroscopy of desert varnishes and their rock substrata. *J. Raman Spectrosc.* 35 475–479.
- Edwards H. G. M., Wynn-Williams D. D. and Jorge-Villar S. E. (2004c): Biological modification of haematite in Antarctic cryptoendolithic communities. *J. Raman Spectrosc.* 35 470–474.
- Edwards H. G. M., Jorge-Villar S. E., Bishop J. L. and Bloomfield M. (2004d): Raman spectroscopy of sediments from the Antarctic Dry Valleys; an analogue study for exploration of potential paleolakes on Mars. *J. Raman Spectrosc.* 35 458–462.
- Edwards H. G. M. and Munshi T. (2005): Diagnostic Raman spectroscopy for the forensic detection of biomaterials and the preservation of cultural heritage. *Anal. Bioanal. Chem.* 382 1398–1406.
- Edwards H. G. M., Jorge-Villar S. E., Parnell J., Cockell C. S. and Lee P. (2005): Raman spectroscopic analysis of cyanobacterial gypsum halotrophs and relevance for sulfate deposits on Mars. *Analyst* 130 917–923.
- Edwards H. G. M., Vandenabeele P., Jorge-Villar S. E., Carter E. A., Rull Perez F. and Hargreaves M. D. (2007a): The Rio Tinto Mars Analogue site: An extremophilic Raman spectroscopic study. *Spectrochimica Acta Part A* 68 1133–1137.
- Edwards H. G. M., Jorge-Villar S. E., Pullan D., Hargreaves M. D., Hofmann B. A. and Westall F. (2007b): Morphological biosignatures from relict fossilised sedimentary geological specimens: a Raman spectroscopic study. *J. Raman Spectrosc.* 38 1352–1361.
- Ellery A., Winn-Williams D. D., Parnell J., Edwards H. G. M. and Dickensheets D. (2004): The role of Raman spectroscopy as an astrobiological tool in the exploration of Mars. *J. Raman Spectroscopy* 35 441–457.
- Erd R. C., White D. E., Fahey J. J. and Lee D. E. (1964): Buddingtonite, an ammonium feldspar with zeolitic water. *Am. Mineral.* 49 831–850.

- Fortes A. D. (2000): Exobiological Implications of a Possible Ammonia–Water Ocean inside Titan. *Icarus* 146 444–452.
- Frost R. L. and Weier M. L. (2003): Raman spectroscopy of natural oxalates at 298 and 77 K. *J. Raman Spectrosc.* 34 776–785.
- Frost R. L. and Weier M. L. (2004): The 'cave' mineral oxammite - a high resolution thermogravimetry and Raman spectroscopic study. *Neues Jahrb. Mineral. Monatsh.* 1 27–48.
- Frost R. L., Kristof J., Rintoul L. and Klopogge J. T. (2000): Raman spectroscopy of urea and urea-intercalated kaolinites at 77 K. *Spectrochim. Acta, Part A* 56 1681–1691.
- Frost R. L., Jing Y. and Ding Z. (2003): Raman and FTIR spectroscopy of natural oxalates: Implications for the evidence of life on Mars. *Chin. Sci. Bull.* 48 1844–1852.
- Frost R. L., Leverett P., Williams P. A., Weier M. L. and Erickson K. L. (2004): Raman spectroscopy of gerhardtite at 298 and 77 K. *J. Raman Spectrosc.* 35 991–996.
- Frost R. L., Weier M. L., Martens W. N., Henry D. A. and Mills S. J. (2005): Raman spectroscopy of newberyite, hannayite and struvite. *Spectrochim. Acta Part A* 62 181–188.
- Frost R. L., Wills R-A., Weier M. L., Martens W. and Klopogge J. T. (2006a): A Raman spectroscopic study of alunites. *J. Mol. Struct.* 785 123–132.
- Frost R. L., Wills R-A., Weier M. L., Martens W. and Mills S. (2006b): A Raman spectroscopic study of selected natural jarosites. *Spectrochim. Acta, Part A* 63 1–8.
- Gandolfo D. and Zarembowitch J. (1977): Coordination of Heterocyclic Compounds in IR and Raman Spectra .3. Spectra of 3-methylpyridine. *Spectrochim. Acta, Part A* 33A 615–623.
- Garavelli A. and Vurro F. (1994): Barberiite, NH_4BF_4 a new mineral from Vulcano, Aeolian Islands, Italy. *Am. Mineral.* 79 381–384.
- Glavin D. P., Dworkin J. P., Aubrey A., Botta O., Doty J. H., Martins Z. and Bada J. L. (2006): Amino acid analyses of Antarctic CM2 meteorites using liquid chromatography-time of flight-mass spectrometry. *Meteorit. Planet. Sci.* 41 889–902.
- Gleadow R. M., Foley W. J. and Woodrow I. E. (1998): Enhanced CO_2 alters the relationship between photosynthesis and defence in cyanogenic *Eucalyptus cladocalyx* F. Muell. *Plant Cell Environ.* 21 12–22.
- Goodwin J. R., Hafner L. M. and Fredericks P. M. (2006): Raman spectroscopic study of the heterogeneity of microcolonies of a pigmented bacterium. *J. Raman Spectrosc.* 37 932–936.
- Grasset O., Sotin C., Deschamps F. (2000): On the internal structure and dynamics of Titan. *Planet. Space Sci.* 48 617–636.
- Gunasekaran S. and Anita B. (2008): Spectral investigation and normal coordinate analysis of piperazine. *Indian J. Pure Appl. Phys.* 46 833–838.
- Gunasekaran S., Anbalagan G. and Pandi S. (2006): Raman and infrares spectra of carbonates of calcite structure. *J. Raman Spectrosc.* 37 892–899.
- Hargreaves M. D., Page K., Munshi T., Tomsett R., Lynch G. and Edwards H. G. M. (2008): Analysis of seized drugs using portable Raman spectroscopy in an airport environment - a proof of principle study. *J. Raman Spectrosc.* 39 873–880.

Hayashi T., Noto T., Nawata Y., Okazaki H., Sawada M. and Ando K. (1982): Cyanocycline A, A new Antibiotic Taxonomy of the Producing organism, Fermentation, Isolation and Characterization. *J. Antibiot.* 35 771–777.

Herbert H.-J., Sander W., Blanke, H., Baitz S., Jacobi H and Follner H. (1995): A new anthropogenic $(K, NH_4)MgCl_3 \cdot 6H_2O$ phase at the location "Bunte First" in the repository for radioactive wastes in Morsleben, Germany. *Neues Jahrb. Mineral. Monatsh.* 8 351–358.

Hester K. C., Dunk R. M., White S. N., Brewer P. G., Peltzer E. T. and Sloan E. D. (2007): Gas hydrate measurements at Hydrate Ridge using Raman spectroscopy. *Geochim. Cosmochim. Acta* 71 2947–2959.

Higashi S. (1982): Tobelite, a new ammonium dioctahedral mica. *Mineral. J.* 11 138–146.

Hori H., Nagashima K., Yamada m., Miyawaki R. and Marubashi T. (1986): Ammonioleucite, a new mineral from Tatarazawa, Fujioka, Japan. *Am. Mineral.* 71 1022–1027.

<http://exploration.esa.int/science-e/www/object/index.cfm?fobjectid=45103> (18. 4. 2011)

http://www.esa.int/SPECIALS/ExoMars/SEM0VIAMS7F_0.html (18. 4. 2011)

Hudson R. L., Moore M. H., Dworkin J. P., Martin M. P. and Pozun Z. D. (2008): Amino Acids from Ion-Irradiated Nitrile-Containing Ices. *Astrobiology* 8 771–779.

Itoh K. and Shimanouchi T. (1972): Vibrational spectra of crystalline formamide. *J. Mol. Spectrosc.* 42 86–99.

Jehlička J. and Culka A. (2010): Raman spectra of nitrogen-containing organic compounds obtained using a portable instrument at $-15\text{ }^{\circ}\text{C}$ at 2860m above sea level. *J. Raman Spectrosc.* 41 537–542.

Jehlička J., Culka A. and Edwards H. G. M. (2010c): Raman spectra of nitrogen containing organic compounds obtained in high altitude sites using a portable spectrometer: Possible application for remote robotic Titan studies. *Planet. Space Sci.* 58 875–881.

Jehlička J., Edwards H. G. M. and Villar S. E. J. (2006): Raman spectroscopic study of mellite - A naturally occurring aluminium benzenhexacarboxylate from lignite - Claystone series of the tertiary age. *Spectrochim. Acta, Part A* 65 229–234.

Jehlička J., Edwards H. G. M. and Villar S. E. J. (2006b): Raman spectroscopic study of mellite - A naturally occurring aluminium benzenhexacarboxylate from lignite - Claystone series of the tertiary age. *Spectrochim. Acta, Part A* 65 229–234.

Jehlička J., Edwards H. G. M., and Culka A. (2010d): Using portable Raman spectrometers for the identification of organic compounds at low temperatures and high altitudes: exobiological applications. *Phil. Trans. R. Soc. A* 368 3109–3125.

Jehlička J., Edwards H. G. M., Villar S. E. J. and Frank O. (2006a): Raman spectroscopic study of the complex aromatic mineral idrialite. *J. Raman Spectrosc.* 37 771–776.

Jehlička J., Edwards H. G. M., Villar S. E. J. and Pokorný J. (2005): Raman spectroscopic study of amorphous and crystalline hydrocarbons from soils, peats and lignite. *Spectrochim. Acta, Part A* 61 2390–2398.

Jehlička J., Vandenabeele P., Edwards H. G. M., Culka A. and Čapoun T. (2010a): Raman spectra of pure biomolecules obtained using a handheld instrument under cold high-altitude conditions. *Anal. Bioanal. Chem.* 397 2753–2760.

Jehlička J., Villar S. E. J. and Edwards H. G. M. (2004): Fourier transform Raman spectra of Czech and Moravian fossil resins from freshwater sediments. *J. Raman Spectrosc.* 35 761–767.

Jehlička J., Vitek P. and Edwards H. G. M. (2010b): Raman spectra of organic acids obtained using a portable instrument at -5 °C in a mountain area at 2000 m above sea level. *J. Raman Spectrosc.* 41 440–444.

Jehlička J., Vitek P., Edwards H. G. M., Heagraves M. D. and Čapoun T. (2009a): Application of portable Raman instruments for fast and non-destructive detection of minerals on outcrops. *Spectrochim. Acta, Part A* 73 410–419.

Jehlička J., Vitek P., Edwards H. G. M., Heagraves M. D. and Čapoun T. (2009b): Fast detection of sulphateminerals (gypsum, anglesite, baryte) by a portable Raman spectrometer. *J. Raman Spectrosc.* 40 1082–1086.

Jehlička J., Vitek P., Edwards H. G. M., Heagraves M. D. and Čapoun T. (2009c): Rapid outdoor non-destructive detection of organic minerals using a portable Raman spectrometer. *J. Raman Spectrosc.* 40 1645–1651.

Jehlička J., Žáček V., Edwards H. G. M., Shcherbakova E. and Moroz T. (2007): Raman spectra of organic compounds kladnoite ($C_6H_4(CO)_2NH$) and hoelite ($C_{14}H_8O_2$)—Rare sublimation products crystallising on self-ignited coal heaps. *Spectrochim. Acta, Part A* 68 1053–1057.

Jorge-Villar S. E. and Edwards H. G. M. (2010): Lichen colonization of an active volcanic environment: a Raman spectroscopic study of extremophile biomolecular protective strategies. *J. Raman Spectrosc.* 41 63–67.

Kelloway S. J., Kononenko N., Torrence R. and Carter E. A. (2010): Assessing the viability of portable Raman spectroscopy for determining the geological source of obsidian. *Vib. Spectrosc.* 53 88–96.

Keuleers R., Desseyn H. O., Rousseau B. and Van Alsenoy C. (1999): Vibrational Analysis of Urea. *J. Phys. Chem. A* 103 4621–4630.

Khare B. N., Sagan C., Ogino H., Nagy B., Cevat E. R., Schram K. H. and Arakawa E. T. (1986): Amino acids derived from Titan tholins. *Icarus* 68 176–184.

Khare B. N., Sagan C., Thompson W. R., Arakawa E. T., Suits F., Callcott T. A., Williams M. W., Shrader S., Ogino H., Willingham T. O. and Nagy B. (1984): The organic aerosols of Titan. *Adv. Space Res.* 4 59–68.

Kharitonov Y. V., Shul'ts E. E., Shakirov M. M. and Tolstikov G. A. (2006): Synthetic Transformations of Higher Terpenoids: XIV.* Heterocyclization Reactions of 15,16,18-Ricarboxylabdadiene. New Nitrogen-Containing Diterpenoids. *Russ. J. Org. Chem.* 42 707–718.

Klingelhofer G., Morris R. V., Bernhardt B., Schroder C., Rodionov D. S., de Souza P. A., Yen A., Gellert R., Evlanov E. N., Zubkov B., Foh J., Bonnes U., Kankeleit E., Gutlich P., Ming D. W., Renz F., Wdowiak T., Squyres S. W. and Arvidson R. E. (2004): Jarosite and hematite at Meridiani Planum from Opportunity's Mossbauer spectrometer. *Science* 306 1740–1745.

Kloprogge J. T. and Frost R. L. (2000): Raman microscopy at 77 K of natural gypsum $CaSO_4$ center dot $2H_2O$. *J. Mater. Sci. Lett.* 19 229–231.

Kloprogge J. T., Broekmans M., Duong L. V., Martens W. N., Hickey L. and Frost R. L. (2006): Low temperature synthesis and characterisation of lecontite, $(NH_4)Na(SO_4) \cdot 2H_2O$. *J. Mater. Sci.* 41 3535–3539.

- Landsberg, G. and Mandelstam L. (1928): Eine neue Erscheinung bei der Lichtzerstreuung in Kristallen. *Naturwissenschaften* 16 557.
- Lautié A., Lautié M. F., Gruger A. and Fakhri S. A. (1980): IR and Raman Spectrometric Analysis of Indole and Indolizine - NH- π Hydrogen-Bond. *Spectrochim. Acta* 36A 85–94.
- Lawrence S. A. (2004): *Amines: Synthesis, Properties and Applications*. Cambridge University Press
- Leavens P. B. (1968): New data on whewellite. *Am. Miner.* 53 455–463.
- Lewis J. S. (2004): *Physics and Chemistry of the Solar System*. International Geophysics Series; vol 87. Elsevier.
- Loughnan F. C., Roberts F. I. and Lindner A. W. (1983): Buddingtonite (NH_4 -feldspar) in the Condor Oilshale Deposit, Queensland, Australia. *Mineral. Mag.* 47 327–334.
- Lunine J. I. and Stevenson D. J. (1987): Clathrate and Ammonia Hydrates at High Pressure: Application to the Origin of Methane on Titan. *Icarus* 70 61–77.
- Madden M. E. E., Bodnar R. J. and Rimstidt J. D. (2004): Jarosite as an indicator of water-limited chemical weathering on Mars. *Nature* 431 821–823.
- Maiman T. H. (1960): Stimulated optical radiation in ruby. *Nature* 187 (4736) 493–494.
- Marshall C. P. and Olcott Marshall A. (2010): The potential of Raman spectroscopy for the analysis of diagenetically transformed carotenoids. *Phil. Trans. R. Soc. A* 368 3137–3144.
- Matlouthi M., Seuvre A-M. and Koenig J. L. (1984): F.t.-i.r. and laser-Raman spectra of thymine and thymidine. *Carbohydr. Res.* 134 23–38.
- Matthews C. N. and Minard R. D. (2006): Hydrogen cyanide polymers, comets and the origin of life. *Faraday Discuss.* 133 393–401.
- McKay C. P. and Smith H. D. (2005): Possibilities for methanogenic life in liquid methane on the surface of Titan. *Icarus* 178 274–276.
- McMurry J. (2008): *Organic Chemistry, Seventh Edition*. Thomson Learning.
- McPherson D. W., Rahman K., Martinez I. and Shevlin P.B. (1987): The formation of amino acid precursors in the reaction of atomic carbon with water and ammonia at 77 K. *Origins Life Evol. Biosphere* 17 275–282.
- Miller S. L. (1953): A production of amino acids under possible primitive earth conditions. *Science* 117 528–529.
- Milton C., Dwornik E. J., Estep-Barnes P. A., Finkelman R. B., Pabst A. and Palmer S. (1978): Abelsonite, nickel porphyrin, a new mineral from the Green River Formation, Utah. *Am. Mineral.* 63 930–937.
- Misra A. K., Sharma S. K., Chio C. H., Lucey P. G. and Lienert B. (2005): Pulsed remote Raman system for daytime measurements of mineral spectra. *Spectrochim. Acta, Part A* 61 2281–2287.
- Mitri G., Showman A. P., Lunine J. I. and Lorenz R. D. (2007): Hydrocarbon lakes on Titan. *Icarus* 186 385–394.
- Moore D. S. and Scharff R. J. (2009): Portable Raman explosives detection. *Anal. Bioanal. Chem.* 393 1571–1578.

Mumma M. J., Villanueva G. L., Novak R. E., Hewagama T., Bonev B. P., DiSanti M. A., Mandell A. M. and Smith M. D. (2009): Strong release of methane on Mars in northern summer 2003. *Science* 323 1041–1045.

Nelson R. M., Kamp L. W., Matson D. L., Irwin P. G. J., Baines K. H., Boryta M. D., Leader F. E., Jaumann R., Smythe W. D., Sotin C., Clark R. N., Cruikshank D. B., Drossart P., Pearl J. C., Hapke B. W., Lunine J., Combes M., Bellucci G., Bibring J.-P., Capaccioni F., Cerroni P., Coradini A., Formisano V., Filacchione G., Langevin R. Y., McCord T. B., Mennella V., Nicholson P. D. and Sicardy B. (2009): Saturn's Titan: Surface change, ammonia, and implications for atmospheric and tectonic activity. *Icarus* 199 429–441.

Niemann H. B., Atreya S. K., Bauer S. J., Carignan G. R., Demick J. E., Frost R. L., Gautier D., Haberman J. A., Harpold D. N., Hunten D. M., Israel G., Lunine J. I., Kasprzak W. T., Owen T. C., Paulkovich M., Raulin F., Raaen E. and Way S.H. (2005): The abundances of constituents of Titan's atmosphere from the GCMS instrument on the Huygens probe. *Nature* 438 779–784.

Osterrothová K. and Jehlička J. (2009): Raman spectroscopic identification of usnic acid in hydrothermal minerals as a potential Martian analogue. *Spectrochim. Acta, Part A* 73 576–580.

Owen T. C., Niemann H., Sushil A. and Zolotov M. Y. (2006): Between heaven and Earth: the exploration of Titan. *Faraday Discuss.* 133 387–391.

Pasteris J., Wopenka B., Freeman J. J., Brewer P. G., White S. N., Peltzer E. T. and Malby G. E. (2004): Raman Spectroscopy in the Deep Ocean: Successes and Challenges. *Appl. Spectrosc.* 58 195A–208A.

Pérez-Alonso M., Castro K. and Madariaga J. M. (2006): Investigation of degradation mechanisms by portable Raman spectroscopy and thermodynamic speciation: The wall painting of Santa María de Lemoniz (Basque Country, North of Spain). *Anal. Chim. Acta* 571 121–128.

Pérez-Alonso M., Castro K., Martínez-Arkarazo I., Angulo M., Olazabal M. A. and Madariaga J. M. (2004): Analysis of bulk and inorganic degradation products of stones, mortars and wall paintings by portable Raman microprobe spectroscopy. *Anal. Bioanal. Chem.* 379 42–50.

Premasiri W. R., Clarke R. H. and Womble M. E. (2001): Urine Analysis by Laser Raman Spectroscopy. *Laser Surg. Med.* 28 330–334.

Raman C. V. and Krishnan K. S. (1928): A New Type of Secondary Radiation. *Nature* 121 501–502.

Rose W. C., Smith L. C., Womack M. and Shane M. (1949): The Utilization of the Nitrogen of Ammonium Salts, Urea, and Certain other Compounds in the Synthesis of Non-essential Amino Acids in vivo. *J. Biol. Chem.* 181 307–316.

Rosemeyer H. (2004): The Chemodiversity of Purine as a Constituent of Natural Products. *Chemistry & Biodiversity* 1 361–401.

Rost R. (1937): *Rozpr. Českosl. Akad. Věd* 47 1.

Rull F., Delgado A. and Martínez-Frías J. (2010): Micro-Raman spectroscopic study of extremely large atmospheric ice conglomerations megacryometeors). *Phil. Trans. R. Soc. A* 368 3145–3152.

- Rull F., Martinez-Frias J., Sansano A., Medina J. and Edwards H. G. M. (2004): Comparative micro-Raman study of the Nakhla and Vaca Muerta meteorites. *J. Raman Spectrosc.* 35 497–503.
- Sagan C. and Khare B. N. (1979): Tholins – Organic chemistry of inter stellar grains and gas. *Nature* 277 102–107.
- Sasaki K., Tanaike O. and Konno H. (1998): Distinction of jarosite-group compounds by Raman spectroscopy. *Can. Mineral.* 36 1225–1235.
- Schaller W. T. (1933): Ammonioborite, a new mineral. *Am. Mineral.* 18 480–492.
- Sharma S. K., Angel S. M., Ghosh M., Hubble H. W. and Lucey P. G. (2002): Remote Pulsed Laser Raman Spectroscopy System for Mineral Analysis on Planetary Surfaces to 66 Meters. *Appl. Spectrosc.* 56 699–705.
- Sharma S. K., Lucey P. G., Ghosh M., Hubble H. W. and Horton K. A. (2003): Stand-off Raman spectroscopic detection of minerals on planetary surfaces. *Spectrochim. Acta, Part A* 59 2391–2407.
- Sharma S. K., Misra A. K. and Sharma B. (2005): Portable remote Raman system for monitoring hydrocarbon, gas hydrates and explosives in the environment. *Spectrochim. Acta, Part A* 61 2404–2412.
- Sharma S. K., Misra A. K., Clegg S. M., Barefield J. E., Wiens R. C. and Acosta T. (2010): Time-resolved remote Raman study of minerals under supercritical CO₂ and high temperatures relevant to Venus exploration. *Philos. Transact. A Math. Phys. Eng. Sci.* 368 3167–3191.
- Schoen C. L., Cooney T. F., Sharma S. K. and Carey D. M. (1992): Long fiber-optic remote Raman probe for detection and identification of weak scatterers. *Appl. Opt.* 31 7707–7715.
- Siemann M. G. (1994): Ammonium bearing carnallite [(K|NH₄)MgCl₃·6H₂O] in the salt mine Marie (Morsleben). *Neues Jahrb. Mineral. Monatsh.* 3 97–100.
- Skinner H. T., Cooney T. F., Sharma S. K. and Angel S. M. (1996): Remote Raman microimaging using an AOTF and a spatially coherent microfiber optical probe. *Appl. Spectrosc.* 50 1007–1014.
- Smith C. H. and Robinson J. D. (1957): Raman Spectra of Formamide-N-d₂ and of Formamide in Concentrated Hydrochloric Acid. *J. Am. Chem. Soc.* 79 1349–1351.
- Söderlund R. and Svensson B. H. (1976): The global nitrogen cycle. In: Svensson B. H., Söderlund R.: Nitrogen, Phosphorus and Sulfur - Global Cycles. - *Econ. Bull.* 22 23–73.
- Stoker C. R., Boston P. J., Mancinelli R. L., Segal W., Khare B. N. and Sagan C. (1990): Microbial Metabolism of Tholin. *Icarus* 85 241–256.
- Stopar J. D., Lucey P. G., Sharma S. K., Misra A. K., Taylor G. J. and Hubble H. W. (2005): Raman efficiencies of natural rocks and minerals: Performance of a remote Raman system for planetary exploration at a distance of 10 meters. *Spectrochimica Acta, Part A* 61 2315–2323.
- Storm C. B., Krane J., Skjetne T., Telnaes N., Branthaver J. F. and Baker E. W. (1984): The Structure of Abelsonite. *Science* 223 1075–1076.
- Thompson W. R., Zollweg J. A. and Gabis D. H. (1992): Vapor-liquid equilibrium thermodynamics of N₂ + CH₄: Model and Titan applications. *Icarus* 97 187–199.

Tobie G., Grasset O., Lunine J. I., Mocquet A. and Sotin C. (2005): Titan's internal structure inferred from a coupled thermal-orbital model. *Icarus* 175 496–502.

Turnbull M. C., Traub W. A., Jucks K. W., Woolf N. J., Meyer M. R., Gorlova N., Skrutskie M. F. and Wilson J. (2006): Spectrum of a habitable world: Earthshine in the near-infrared. *Astrophys. J.* 644 551–559.

Vandenabeele P., Tate J. and Moens L. (2007): Non-destructive analysis of museum objects by fibre-optic Raman spectroscopy. *Anal. Bioanal. Chem.* 387 813–819.

Vítek P., Jehlička J., Edwards H. G. M. and Osterrothová K. (2009a): Identification of beta-carotene in an evaporitic matrix-evaluation of Raman spectroscopic analysis for astrobiological research on Mars. *Anal. Bioanal. Chem.* 393 1967–1975.

Vítek P., Osterrothová K. and Jehlička J. (2009): Beta-carotene—A possible biomarker in the Martian evaporitic environment: Raman micro-spectroscopic study. *Planet. Space Sci.* 57 454–459.

Vítek P., Edwards H. G. M., Jehlička J., Ascaso C., De los Rios A., Valea S., Jorge-Villar S. E., Davila A. F. and Wierzchos J. (2010): Microbial colonization of halite from the hyper-arid Atacama Desert studied by Raman spectroscopy. *Phil. Trans. R. Soc. A* 368 3205–3221.

Wang A., Freeman J. J., Jolliff B. L. and Chou I-Ming. (2006): Sulfates on Mars: A systematic Raman spectroscopic study of hydration states of magnesium sulfates. *Geochim. Cosmochim. Acta* 70 6118–6135.

Wang A., Kuebler K., Jolliff B. and Haskin L. A. (2004): Mineralogy of a Martian meteorite as determined by Raman spectroscopy. *J. Raman Spectrosc.* 35 504–514.

White S. N., Dunk R. M., Peltzer E. T., Freeman J. J. and Brewer P. G. (2006): In situ Raman analyses of deep-sea hydrothermal and cold seep systems (Gorda Ridge and Hydrate Ridge). *Geochem. Geophys. Geosyst.* 7 Article Number: Q05023

White S. N., Kirkwood W., Sherman A., Brown M., Henthorn R., Salamy K., Walz P., Peltzer E. T. and Brewer P. G. (2005): Development and deployment of a precision underwater positioning system for in situ laser Raman spectroscopy in the deep ocean. *Deep Sea Res. Part I* 52 2376–2389.

Wilson R., Monaghan P., Bowden S. A., Parnell J and Cooper J. M. (2007): Surface-Enhanced Raman Signatures of Pigmentation of Cyanobacteria from within Geological Samples in a Spectroscopic-Microfluidic Flow Cell. *Anal. Chem.* 79 7036–7041.

Winchell H. and Benoit J. (1951): Taylorite, mascagnite, aphthitalite, lecontite, and oxammite from guano. *Am. Miner.* 36 590–602.

Yan F. and Vo-Dinh T. (2007): Surface-enhanced Raman scattering detection of chemical and biological agents using a portable Raman integrated tunable sensor. *Sens. Actuators, B* 121 61–66.